Table 3
Comparison of specific MF of Spi$^-$ mutations between *gpt* delta mice and GDL1 cells

Type of mutation	Class of mutation	Control			MMC			
		gpt delta mice[a]	GDL1 cells		*gpt* delta mice[a]		GDL1 cells	
		Specific MF[b] ($\times 10^{-6}$)	Specific MF[b] ($\times 10^{-6}$)	*P* value[c,d]	Specific MF[b] ($\times 10^{-6}$)	*P* value[c,e]	Specific MF[b] ($\times 10^{-6}$)	*P* value[c,f]
Large deletion (>1 kbp)								
With microhomology	I-A	0.0	4.2	<0.0001	1.6	<0.001	17.6	<0.01
Without microhomology	I-B	0.1	0.0	1.00	0.6	0.19	5.9	<0.05
Midsize deletion (2 bp to 1 kbp)	II	0.0	1.2	<0.05	0.2	0.47	7.8	<0.05
Single base deletion								
At run sequence	III-A	1.4	17.3	<0.0001	1.4	1.00	33.2	0.06
At non-run sequence	III-B	0.1	1.2	0.08	0.2	1.00	0.0	1.00
Complex mutation	IV	0.0	0.0	–	0.0	–	9.8	<0.001
Miscellaneous mutation	V	0.1	1.8	<0.05	1.3	<0.05	11.7	<0.01
Unidentified		0.0	0.0	–	0.0	–	2.0	0.24
Total		1.8	25.6	<0.0001	5.2	<0.01	88.0	<0.0001

[a] Data previously reported by us [8].
[b] Specific MF was calculated by multiplying the total mutation frequency by the ratio of each type of mutation to the total mutation.
[c] *P* values were determined using Fisher's exact test according to Carr and Gorelick [22].
[d] Comparison between the control group of *gpt* delta mice and control group of GDL1 cells.
[e] Comparison between the control group of *gpt* delta mice and MMC-treated group of *gpt* delta mice.
[f] Comparison between the control group of GDL1 cells and MMC-treated group of GDL1 cells.

expressed [36]. Thus, a p53 defect by the recombinant SV40 T antigen may cause the DNA rearrangement occurring in GDL1 cells. The breakage-fusion bridge cycle reported in p53 deficient mammalian cells might involve in the DNA rearrangement observed in GDL1 cells [37,38].

It is interesting and surprising to note that Spi$^-$ mutant sM1-9 has a DNA fragment from chromosome

Table 4
Comparison of specific MF of *gpt* mutations between *gpt* delta mice and GDL1 cells

Type of mutation	Control			MMC			
	gpt delta mice[a]	GDL1 cells		*gpt* delta mice[a]		GDL1 cells	
	Specific MF[b] ($\times 10^{-6}$)	Specific MF[b] ($\times 10^{-6}$)	*P* value[c,d]	Specific MF[b] ($\times 10^{-6}$)	*P* value[c,e]	Specific MF[b] ($\times 10^{-6}$)	*P* value[c,f]
Base substitution/single							
At G:C	5.4	10.9	<0.05	6.6	0.47	40.3	<0.0001
At A:T	1.7	5.9	<0.01	1.9	0.75	5.3	1.00
Insertion	0.0	2.5	<0.01	0.0	–	7.0	0.12
Deletion	1.1	3.0	0.10	0.9	0.30	10.5	<0.05
Base substitution/tandem	0.0	0.0	–	3.3	<0.001	8.8	<0.001
Others	0.0	0.5	0.35	1.4	<0.05	7.0	<0.05
Total	8.2	22.7	<0.0001	14.1	<0.0001	78.9	<0.0001

[a] Data previously reported by us [8].
[b] Specific MF was calculated by multiplying the total mutation frequency by the ratio of each type of mutation to the total mutation.
[c] *P* values were determined using Fisher's exact test according to Carr and Gorelick [22].
[d] Comparison between the control group of *gpt* delta mice and control group of GDL1 cells.
[e] Comparison between the control group of *gpt* delta mice and MMC-treated group of *gpt* delta mice.
[f] Comparison between the control group of GDL1 cells and MMC-treated group of GDL1 cells.

16 (Fig. 5). Since DNA double strand breaks (DSBs)-containing chromosome domains are mobile [39], the DNA fragment of chromosome 16 might migrate to the breakage site of chromosome 17 where the *red/gam* reporter genes are present. Although further investigations are required to reveal the precise mechanisms by which DNA rearrangements are induced by MMC, the results strongly suggest that GDL1 cells are useful to investigate the molecular mechanisms of translocations induced by chromosome instability.

An intriguing feature of GDL1 cells is the higher spontaneous frequencies in the Spi$^-$ and *gpt* mutations compared to those of *gpt* delta mice (Tables 3 and 4). The spontaneous Spi$^-$ MFs in *gpt* delta mice are 1.1×10^{-6} in epidermis [12], 1.3×10^{-6} to 1.8×10^{-6} in bone marrow [7,8], 1.8×10^{-6} in spleen, 2.2×10^{-6} in liver, 2.4×10^{-6} in testis, and 2.6×10^{-6} in kidney [9]. Since spontaneous MF of Spi$^-$ selection in GDL1 cells was 25.6×10^{-6} (Table 3), it is 9.8–23-fold higher than the MFs in the organs of mice. Similarly, the spontaneous *gpt* MFs in *gpt* delta mice are 2.4×10^{-6} to 6.6×10^{-6} in liver [9,40], 6.0×10^{-6} in lung [41], 6.2×10^{-6} to 9.0×10^{-6} in colon [40,42], 8.2×10^{-6} in bone marrow [8], 12.1×10^{-6} in dermis, and 13.4×10^{-6} in epidermis [11]. The spontaneous MF of 6-TG selection in GDL1 cells was 22.7×10^{-6} (Table 4). The value is 1.7–9.5-fold higher than the MFs in various organs of *gpt* delta mice. In particular, the specific MF of class I mutations of Spi$^-$ (large deletions of a size more than 1 kbp) was more than 40 times higher in vitro (4.2×10^{-6}) than in vivo (0.1×10^{-6}) (Table 3). Even when we eliminated all possible clonally expanded class I mutants (Fig. 4), the specific MF was still about 20 times higher in GDL1 cells than in *gpt* delta mice. Single base deletions, i.e., class III mutants, also are more than 10 times higher in vitro (18.5×10^{-6}) than in vivo (1.5×10^{-6}). Most large deletions and single base deletions are probably due to the nonhomologous end-joining of DSBs in DNA and slippage errors during DNA replication, respectively. Thus, we suggest that spontaneous DNA strand breaks and slippage errors are more frequently induced in vitro than in vivo. Higher rates of cell proliferation in vitro compared with in vivo may be one reason for the higher incidence of DSBs and slippage errors in GDL1 cells.

Likewise, differences between in vitro and in vivo were seen in single base insertions and single base deletions in the spontaneous *gpt* mutations (Table 4). Eleven of forty-six (24%) mutations were single base insertions or small deletions in spontaneous *gpt* mutants in GDL1 cells (Table 2), and seven of them (7/11 = 64%) occurred in the DNA sequence in the run of the identical nucleotide (Fig. 6). On the contrary, in the *gpt* delta mice, 4 of 29 mutations (14%) were single base deletions, and the mutations were not observed in the run of the identical nucleotide [8]. Not only in our cell lines but also in other cell lines having different lambda shuttle vectors for detection of mutations, insertions/deletions tend to be higher than those observed in the transgenic animals from which the cells originated [43–45]. Therefore, higher induction of deletion/insertion mutations is generally observed in cell lines carrying lambda shuttle vectors compared with in vivo. This tendency is expected to affect the increase in spontaneous MF more severely in Spi$^-$ selection than in 6-TG selection because Spi$^-$ selection is more sensitive to deletion/insertion mutations than 6-TG selection. In fact, the increase in spontaneous MFs was higher in Spi$^-$ selection (9.8–23-fold) than in 6-TG selection (1.7–9.5-fold) when compared between in vitro and in vivo as described above.

The combination of a lambda shuttle vector and a reporter gene is one of the most effective tools presently applicable for mutation analysis. Several cell lines have been established from TG mouse strains harboring the lambda vector system. Big Blue Rat2 [46], Big Blue mouse embryonic fibroblast cell lines [47], BBR/ME, BBR/OE, and BBR/MFib [48] are immortalized cell lines carrying *lacI* shuttle vectors. BBR1 and BBM1 are primary cultured cell lines from *lacI* transgenic mice [49]. EF1 is a cell line derived from *lacZ* transgenic mice [50]. However, the parent animals were insensitive to the MMC treatment or X-ray irradiation that effectively induces deletions [51,52]. Induction of large deletion mutations in these cells has not been reported. The sizes of the reporter genes are approximately 1 kbp in *lacI*, 3 kbp in *lacZ*, and 0.3 kbp in *cII* [2]. It may be difficult to detect large deletion mutations larger than the reporter genes. Additionally, highly predominant induction of base substitution mutations may hide an increase in deletion mutations because both the *lacI* and *lacZ* systems detect both point mutations and deletion mutations in a single selection system. Therefore, the result in the present study that GDL1 cells detected large deletion mutations suggests a distinct advantage.

It is common to use some agents that accelerate and/or accumulate mutations to establish a cell line from an animal tissue. A majority of the cell lines from the lambda vector TG rodent strains were established after treatment with strong mutagens for the purpose of immortalizing the cells. X-ray and benzo[*a*]pyrene were used for the Big Blue mouse embryonic fibroblast cell line [47]. *N*-Ethyl-*N*-nitrosourea was used for BBR/ME, BBR/OE, and BBR/MFib [48]. However, the SV40 T antigen gene was used to establish the GDL1 cells. This is the first attempt to apply the SV40 T antigen to the cell lines

for genotoxicity assays. Information on the biological functions of the SV40 T antigen may support better understanding of the responses of GDL1 cells to mutagens. The normal functions of p53 were lost in the CHL, CHO, and L5178Y $tk^{+/-}$ cells, which are commonly used in genotoxicity tests [53,54]. The dysfunction of p53 prevents the cells from apoptosis when the cells are damaged by mutagens. Since p53 plays an important role in DNA repair and genome stability, the dysfunction of the protein may increase the genetic damage by mutagens.

The present study demonstrates that the established GDL1 cell line detected large deletion mutations induced by MMC. The GDL1 cell is a useful tool for detecting various mutations including large deletion mutations, which covers all types of mutations induced in *gpt* delta mice. Although there are two differences in mutation spectra, i.e., single base substitution and complex rearrangement, between GDL1 cells and *gpt* delta mice after MMC treatment, the mutations detected in GDL1 cells are generally consistent with observations in *gpt* delta mice. A combination of GDL1 cell and gene targeting techniques, such as siRNA, knockout, or overexpression of target genes, may be an informative approach to understanding intracellular procedures involved in mutation and DNA repair.

Acknowledgement

This work was supported by a grant-in-aid from the Japan Health Science Foundation (MI and TN).

References

[1] C.J. Shaw, J.R. Lupski, Implications of human genome architecture for rearrangement-based disorders: the genomic basis of disease, Hum. Mol. Genet. 13 (2004) 57–64.

[2] T. Nohmi, T. Suzuki, K. Masumura, Recent advances in the protocols of transgenic mouse mutation assays, Mutat. Res. 455 (2000) 191–215.

[3] J.A. Heddle, S. Dean, T. Nohmi, M. Boerrigter, D. Casciano, G.R. Douglas, B.W. Glickman, N.J. Gorelick, J.C. Mirsalis, H.J. Martus, T.R. Skopek, V. Thybaud, K.R. Tindall, N. Yajima, *In vivo* transgenic mutation assays, Environ. Mol. Mutagen. 35 (2000) 253–259.

[4] T. Nohmi, M. Katoh, H. Suzuki, M. Matsui, M. Yamada, M. Watanabe, M. Suzuki, N. Horiya, O. Ueda, T. Shibuya, H. Ikeda, T. Sofuni, A new transgenic mouse mutagenesis test system using Spi⁻ and 6-thioguanine selections, Environ. Mol. Mutagen. 28 (1996) 465–470.

[5] J.A. Gossen, H.J. Martus, J.Y. Wei, J. Vijg, Spontaneous and X-ray-induced deletion mutations in a *LacZ* plasmid-based transgenic mouse model, Mutat. Res. 331 (1995) 89–97.

[6] H. Louro, M.J. Silva, M.G. Boavida, Mutagenic activity of cisplatin in the *lacZ* plasmid-based transgenic mouse model, Environ. Mol. Mutagen. 40 (2002) 283–291.

[7] N. Okada, K. Masumura, T. Nohmi, N. Yajima, Efficient detection of deletions induced by a single treatment of mitomycin C in transgenic mouse *gpt* delta using the Spi⁻ selection, Environ. Mol. Mutagen. 34 (1999) 106–111.

[8] A. Takeiri, M. Mishima, K. Tanaka, A. Shioda, O. Ueda, H. Suzuki, M. Inoue, K. Masumura, T. Nohmi, Molecular characterization of mitomycin C-induced large deletions and tandem-base substitutions in the bone marrow of *gpt* delta transgenic mice, Chem. Res. Toxicol. 16 (2003) 171–179.

[9] K. Masumura, K. Kuniya, T. Kurobe, M. Fukuoka, F. Yatagai, T. Nohmi, Heavy-ion-induced mutations in the *gpt* delta transgenic mouse: comparison of mutation spectra induced by heavy-ion, X-ray, and gamma-ray radiation, Environ. Mol. Mutagen. 40 (2002) 207–215.

[10] T. Nohmi, M. Suzuki, K. Masumura, M. Yamada, K. Matsui, O. Ueda, H. Suzuki, M. Katoh, H. Ikeda, T. Sofuni, Spi⁻ selection: an efficient method to detect gamma-ray-induced deletions in transgenic mice, Environ. Mol. Mutagen. 34 (1999) 9–15.

[11] M. Horiguchi, K. Masumura, H. Ikehata, T. Ono, Y. Kanke, T. Sofuni, T. Nohmi, UVB-induced *gpt* mutations in the skin of *gpt* delta transgenic mice, Environ. Mol. Mutagen. 34 (1999) 72–79.

[12] M. Horiguchi, K.I. Masumura, H. Ikehata, T. Ono, Y. Kanke, T. Nohmi, Molecular nature of ultraviolet B light-induced deletions in the murine epidermis, Cancer Res. 61 (2001) 3913–3918.

[13] D.C. Doll, R.B. Weiss, B.F. Issell, Mitomycin: ten years after approval for marketing, J. Clin. Oncol. 3 (1985) 276–286.

[14] M. Tomasz, Y. Palom, The mitomycin bioreductive antitumor agents: cross-linking and alkylation of DNA as the molecular basis of their activity, Pharmacol. Ther. 76 (1997) 73–87.

[15] M. Tomasz, R. Lipman, D. Chowdary, J. Pawlak, G.L. Verdine, K. Nakanishi, Isolation and structure of a covalent cross-link adduct between mitomycin C and DNA, Science 235 (1987) 1204–1208.

[16] M. Tomasz, A.K. Chawla, R. Lipman, Mechanism of monofunctional and bifunctional alkylation of DNA by mitomycin C, Biochemistry 27 (1988) 3182–3187.

[17] K.G. Suresh, R. Lipman, J. Cummings, M. Tomasz, Mitomycin C-DNA adducts generated by DT-diaphorase. Revised mechanism of the enzymatic reductive activation of mitomycin C, Biochemistry 36 (1997) 14128–14136.

[18] Y. Palom, R. Lipman, S.M. Musser, M. Tomasz, A mitomycin-N^6-deoxyadenosine adduct isolated from DNA, Chem. Res. Toxicol. 11 (1998) 203–210.

[19] Y. Palom, M.F. Belcourt, S.M. Musser, A.C. Sartorelli, S. Rockwell, M. Tomasz, Structure of adduct X, the last unknown of the six major DNA adducts of mitomycin C formed in EMT6 mouse mammary tumor cells, Chem. Res. Toxicol. 13 (2000) 479–488.

[20] H. Ariga, S. Sugano, Initiation of simian virus 40 DNA replication in vitro, J. Virol. 48 (1983) 481–491.

[21] J.H. Bielas, J.A. Heddle, Proliferation is necessary for both repair and mutation in transgenic mouse cells, Proc. Natl. Acad. Sci. U.S.A. 97 (2000) 11391–11396.

[22] G.J. Carr, N.J. Gorelick, Mutational spectra in transgenic animal research: data analysis and study design based upon the mutant or mutation frequency, Environ. Mol. Mutagen. 28 (1996) 405–413.

[23] A.K. Basu, C.J. Hanrahan, S.A. Malia, S. Kumar, R. Bizanek, M. Tomasz, Effect of site-specifically located mitomycin C-DNA monoadducts on in vitro DNA synthesis by DNA polymerases, Biochemistry 32 (1993) 4708–4718.

[24] V.-S. Li, H. Kohn, Studies on the bonding specificity for mitomycin C-DNA monoalkylation processes, J. Am. Chem. Soc. 113 (1991) 275–283.

[25] N.S. Srikanth, A. Mudipalli, A.E. Maccubbin, H.L. Gurtoo, Mutations in a shuttle vector exposed to activated mitomycin C, Mol. Carcinog. 10 (1994) 23–29.
[26] A.E. Maccubbin, A. Mudipalli, S.S. Nadadur, N. Ersing, H.L. Gurtoo, Mutations induced in a shuttle vector plasmid exposed to monofunctionally activated mitomycin C, Environ. Mol. Mutagen. 29 (1997) 143–151.
[27] P.S. Jat, P.A. Sharp, Cell lines established by a temperature-sensitive simian virus 40 large-T-antigen gene are growth restricted at the nonpermissive temperature, Mol. Cell. Biol. 9 (1989) 1672–1681.
[28] J.M. Ruppert, B. Stillman, Analysis of a protein-binding domain of p53, Mol. Cell. Biol. 13 (1993) 3811–3820.
[29] R.S. Quartin, C.N. Cole, J.M. Pipas, A.J. Levine, The amino-terminal functions of the simian virus 40 large T antigen are required to overcome wild-type p53-mediated growth arrest of cells, J. Virol. 68 (1994) 1334–1341.
[30] S.M. Morris, A role for p53 in the frequency and mechanism of mutation, Mutat. Res. 511 (2002) 45–62.
[31] P.C. Hanawalt, Controlling the efficiency of excision repair, Mutat. Res. 485 (2001) 3–13.
[32] S. Adimoolam, J.M. Ford, p53 and regulation of DNA damage recognition during nucleotide excision repair, DNA Repair 2 (2003) 947–954.
[33] P.C. Hanawalt, J.M. Ford, D.R. Lloyd, Functional characterization of global genomic DNA repair and its implications for cancer, Mutat. Res. 544 (2003) 107–114.
[34] K.K. Bowman, D.M. Sicard, J.M. Ford, P.C. Hanawalt, Reduced global genomic repair of ultraviolet light-induced cyclobutane pyrimidine dimers in simian virus 40-transformed human cells, Mol. Carcinog. 29 (2000) 17–24.
[35] J.M. Ford, E.L. Baron, P.C. Hanawalt, Human fibroblasts expressing the human papillomavirus E6 gene are deficient in global genomic nucleotide excision repair and sensitive to ultraviolet irradiation, Cancer Res. 58 (1998) 599–603.
[36] F. Yatagai, T. Kurobe, T. Nohmi, K. Masumura, T. Tsukada, H. Yamaguchi, K. Kasai-Eguchi, N. Fukunishi, Heavy-ion-induced mutations in the *gpt* delta transgenic mouse: effect of p53 gene knockout, Environ. Mol. Mutagen. 40 (2002) 216–225.
[37] C. Zhu, K.D. Mills, D.O. Ferguson, C. Lee, J. Manis, J. Fleming, Y. Gao, C.C. Morton, F.W. Alt, Unrepaired DNA breaks in p53-deficient cells lead to oncogenic gene amplification subsequent to translocations, Cell 109 (2002) 811–821.
[38] M. Honma, M. Izumi, M. Sakuraba, S. Tadokoro, H. Sakamoto, W. Wang, F. Yatagai, M. Hayashi, Deletion, rearrangement, and gene conversion; genetic consequences of chromosomal double-strand breaks in human cells, Environ. Mol. Mutagen. 42 (2003) 288–298.
[39] J.A. Aten, J. Stap, P.M. Krawczyk, C.H. van Oven, R.A. Hoebe, J. Essers, R. Kanaar, Dynamics of DNA double-strand breaks revealed by clustering of damaged chromosome domains, Science 303 (2004) 92–95.
[40] K. Masumura, Y. Totsuka, K. Wakabayashi, T. Nohmi, Potent genotoxicity of aminophenylnorharman, formed from non-mutagenic norharman and aniline, in the liver of *gpt* delta transgenic mouse, Carcinogenesis 24 (2003) 1985–1993.
[41] A.H. Hashimoto, K. Amanuma, K. Hiyoshi, H. Takano, K. Masumura, T. Nohmi, Y. Aoki, In vivo mutagenesis induced by benzo[*a*]pyrene instilled into the lung of *gpt* delta transgenic mice, Environ. Mol. Mutagen. 45 (2005) 365–373.
[42] K. Masumura, M. Horiguchi, A. Nishikawa, T. Umemura, K. Kanki, Y. Kanke, T. Nohmi, Low dose genotoxicity of 2-amino-3,8-dimethylimidazo[4,5-*f*]quinoxaline (MeIQx) in *gpt* delta transgenic mice, Mutat. Res. 541 (2003) 91–102.
[43] C.N. Sprung, Y.P. Wang, D.L. Miller, D.D. Giannini, N. Dhananjaya, W.J. Bodell, Induction of *lacI* mutations in Big Blue Rat-2 cells treated with 1-(2-hydroxyethyl)-1-nitrosourea: a model system for the analysis of mutagenic potential of the hydroxyethyl adducts produced by 1,3-bis (2-chloroethyl)-1-nitrosourea, Mutat. Res. 484 (2001) 77–86.
[44] D.M. Zimmer, X.B. Zhang, P.R. Harbach, J.K. Mayo, C.S. Aaron, Spontaneous and ethylnitrosourea-induced mutation fixation and molecular spectra at the *lacI* transgene in the Big Blue rat-2 embryo cell line, Environ. Mol. Mutagen. 28 (1996) 325–333.
[45] J.C. Ryu, Y.J. Kim, Y.G. Chai, Mutation spectrum of 1,2-dibromo-3-chloropropane, an endocrine disruptor, in the *lacI* transgenic Big Blue Rat2 fibroblast cell line, Mutagenesis 17 (2002) 301–307.
[46] D.L. Wyborski, S. Malkhosyan, J. Moores, M. Perucho, J.M. Short, Development of a rat cell line containing stably integrated copies of a lambda/*lacI* shuttle vector, Mutat. Res. 334 (1995) 161–165.
[47] G.L. Erexson, M.L. Cunningham, K.R. Tindall, Cytogenetic characterization of the transgenic Big Blue Rat2 and Big Blue mouse embryonic fibroblast cell lines, Mutagenesis 13 (1998) 649–653.
[48] H.M. McDiarmid, G.R. Douglas, B.L. Coomber, P.D. Josephy, Epithelial and fibroblast cell lines cultured from the transgenic BigBlue rat: an in vitro mutagenesis assay, Mutat. Res. 497 (2001) 39–47.
[49] G.L. Erexson, D.E. Watson, K.R. Tindall, Characterization of new transgenic Big Blue® mouse and rat primary fibroblast cell strains for use in molecular toxicology studies, Environ. Mol. Mutagen. 34 (1999) 90–96.
[50] P.A. White, G.R. Douglas, J. Gingerich, C. Parfett, P. Shwed, V. Seligy, L. Soper, L. Berndt, J. Bayley, S. Wagner, K. Pound, D. Blakey, Development and characterization of a stable epithelial cell line from Muta Mouse lung, Environ. Mol. Mutagen. 42 (2003) 166–184.
[51] T. Suzuki, M. Hayashi, T. Sofuni, B.C. Myhr, The concomitant detection of gene mutation and micronucleus induction by mitomycin C in vivo using *lacZ* transgenic mice, Mutat. Res. 285 (1993) 219–224.
[52] K.S. Tao, C. Urlando, J.A. Heddle, Comparison of somatic mutation in a transgenic versus host locus, Proc. Natl. Acad. Sci. U.S.A. 90 (1993) 10681–10685.
[53] T. Hu, C.M. Miller, G.M. Ridder, M.J. Aardema, Characterization of p53 in Chinese hamster cell lines CHO-K1, CHO-WBL, and CHL: implications for genotoxicity testing, Mutat. Res. 426 (1999) 51–62.
[54] R.D. Storer, A.R. Kraynak, T.W. McKelvey, M.C. Elia, T.L. Goodrow, J.G. DeLuca, The mouse lymphoma L5178Y $Tk^{+/-}$ cell line is heterozygous for a codon 170 mutation in the p53 tumor suppressor gene, Mutat. Res. 373 (1997) 157–165.

Deletion and single nucleotide substitution at G:C in the kidney of *gpt* delta transgenic mice after ferric nitrilotriacetate treatment

Li Jiang,[1] Yi Zhong,[1] Shinya Akatsuka,[1] Yu-Ting Liu,[1] Khokon Kumar Dutta,[1] Wen-Hua Lee,[1] Janice Onuki,[1,2] Ken-ichi Masumura,[3] Takehiko Nohmi[3] and Shinya Toyokuni[1,4]

[1]Department of Pathology and Biology of Diseases, Graduate School of Medicine, Kyoto University, Kyoto 606-8501; [2]Laboratory of Biochemistry and Biophysics, Butantan Institute, São Paulo, SP, Brazil; [3]Division of Genetics and Mutagenesis, National Institute of Health Sciences, Tokyo 158-8501, Japan

(Received June 7, 2006/Revised July 13, 2006/Accepted July 14, 2006/Online publication August 23, 2006)

An iron chelate, ferric nitrilotriacetate (Fe-NTA), induces oxidative renal proximal tubular damage that subsequently leads to a high incidence of renal cell carcinoma in rodents, presenting an intriguing model of free radical-induced carcinogenesis. In the present study, we used *gpt* delta transgenic mice, which allow efficient detection of point mutations and deletions *in vivo*, to evaluate the mutation spectra, in association with the formation of 8-oxoguanine and acrolein-modified adenine during the first 3 weeks of carcinogenesis. Immunohistochemical analysis revealed the highest levels of 8-oxoguanine and acrolein-modifed adenine in the renal proximal tubules after 1 week of repeated administration. DNA immunoprecipitation and quantitative polymerase chain reaction analysis showed that the relative abundance of 8-oxoguanine and acrolein-modified adenine at the *gpt* reporter gene were increased at the first week in the kidney. Similarly, in both 6-thioguanine and Spi$^-$ selections performed on the renal specimens after Fe-NTA administration, the mutant frequencies were increased in the Fe-NTA-treated mice at the first week. Further analyzes of 79 mutant clones and 93 positive plaques showed a high frequency of G:C pairs as preferred targets for point mutation, notably G:C to C:G transversion-type mutation followed by deletion, and of large-size (>1 kilobase) deletions with short homologous sequences in proximity to repeated sequences at the junctions. The results demonstrate that the iron-based Fenton reaction is mutagenic *in vivo* in the renal tubular cells and induces characteristic mutations. (*Cancer Sci* 2006; 97: 1159–1167)

Oxidative stress is associated with a variety of pathological phenomena, including infection, inflammation, ultraviolet- and γ-irradiation, overload of transition metals and certain chemical agents.[1] Many epidemiological studies have demonstrated a close association between chronically oxidative conditions and carcinogenesis. For example, chronic tuberculous pleuritis causes a high incidence of malignant lymphoma;[2] asbestosis (asbestos fibers are rich in iron),[3] is often associated with mesothelioma and lung carcinoma;[4] chronic *Helicobacter pylori* infection is associated with a high incidence of gastric cancer;[5,6] the incidence of colorectal cancer is increased in ulcerative colitis;[7,8] a high risk for heptocellular carcinoma is observed in patients with genetic hemochromatosis, an iron overload disease;[9,10] severe burns by ultraviolet radiation is a risk factor for skin cancer;[11,12] and γ-irradiation causes a high incidence of leukemia.[13] At least under these circumstances, and probably in other types of carcinogenesis as well, oxidative stress appears to play a major role in human carcinogenesis.

An iron chelate, ferric nitrilotriacetate (Fe-NTA), causes oxidative renal proximal tubular injury via the Fenton reaction, and this injury ultimately leads to a high incidence of renal cell carcinoma in mice[14] and rats[15] after repeated intraperitoneal administration. This is an intriguing model in the following respects: (1) more than half of the induced tumors metastasize to the lung and/or invade the peritoneal cavity, resulting in animal mortality;[16] (2) convincing evidence exists regarding the involvement of free radical reactions in the carcinogenic process, including not only an increase in covalently modified macromolecules (oxidatively modified DNA bases[17] and lipid peroxidation products)[18,19] but also preventive effects of α-tocopherol fortification against carcinogenesis;[20] (3) genetic changes in the $p16^{INK4a}$ tumor suppressor gene, especially homozygous deletions[21,22] and expressional alteration of several key genes, including annexin 2[23] and thioredoxin binding protein-2,[24] have been observed.

Fe-NTA itself is Ames test-negative,[14] but is positive in other cell culture systems detecting mutations.[25,26] Thus far, its mutation spectrum has not been comprehensively studied. Since the Ames test is a system involving prokaryotes, an assay system with the ability to detect mutations under *in vivo* conditions in which eukaryotic DNA repair mechanisms, metabolic pathways and other physiological systems are operative would offer significant advantages with respect to reliability. Based on this premise, several transgenic mouse mutagenesis assay systems have been developed, including Muta mice,[27] Big Blue mice[28] and HITEC mice.[29] These systems employ a recoverable transgenic lambda phage vector containing a reporter gene from bacteria. However, these systems all have the limitation that large deletions cannot be efficiently detected. We have developed a novel mutagenesis test system named *gpt* delta transgenic mice, which are transgenic for the *lambda EG 10* gene containing the *gpt* gene of *Escherichia coli*.[30] An important feature of this system is that both point mutations and large deletions can be tested concurrently in the targeted organs of the mice; point mutations are detected by 6-thioguanine (6-TG) selection and deletions larger than 1 kb can be identified by Spi$^-$ (sensitive to P2 interference) selection. Thus far, various mutagens, including γ-ray irradiation, UVB, mitomycin C and PhIP, have been studied by using this *in vivo* system.[31]

In the present study, we used *gpt* transgenic mice to investigate the early genetic changes in Fe-NTA-induced renal carcinogenesis. Furthermore, we studied the relative abundance of two different types of DNA base modifications in several limited genomic loci with a novel technique called DNA immunoprecipitation (DnaIP), which selectively collects enzyme-digested DNA fragments

*To whom correspondence should be addressed.
E-mail: toyokuni@path1.med.kyoto-u.ac.jp
Abbreviations: acrolein-dA, acrolein-modified 2′-deoxyadenosine; APNH, aminophenylnorharman; bp, base pairs; Cm, chloramphenicol; dCTP, 2′-deoxycytidine triphosphate; DnaIP, DNA immunoprecipitation; EDTA, ethylenediaminetetraacetic acid; FaPy, formamidopyrimidine; Fe-NTA, ferric nitrilotriacetate; MF, mutant frequency; MMC, mitomycin C; 8-OHdG, 8-hydroxy-2′-deoxyguanosine; PCR, polymerase chain reaction; PhIP, 2-amino-1-methyl-6-phenylimidazo[4,5-b]pyridine; 6-TG, 6-thioguanine; UVB, ultraviolet B; TE, Tris-EDTA.

doi: 10.1111/j.1349-7006.2006.00301.x

containing the target oxidative DNA base modification with specific monoclonal antibody. The present study for the first time revealed characteristics of the mutation spectrum in the kidney following repeated episodes of the Fenton reaction.

Materials and Methods

Animals and chemicals. *Gpt* delta C57BL/6 J transgenic mice were provided by Dr Takehiko Nohmi (Division of Genetics and Mutagenesis, National Institute of Health Sciences, Tokyo, Japan) and maintained in Kyoto University under specific-pathogen free and light-, temperature- and humidity-controlled conditions. The animal experiment committee of the Graduate School of Medicine, Kyoto University, approved the present experiments. $Fe(NO_3)_3 9H_2O$ was obtained from Wako (Osaka, Japan). Nitrilotriacetic acid, disodium salt, was purchased from Nacalai Tesque (Kyoto, Japan). Fe-NTA was prepared immediately before use as described previously.[18] A total of 12 4-week-old male mice were used; nine mice were subjected to repetitive Fe-NTA administration and three mice were used as untreated controls. Mice were injected intraperitoneally with 3 mg iron/kg of Fe-NTA daily for three days, and the dose was increased to 5 mg iron/kg of Fe-NTA from the fourth day according to the established carcinogenesis protocol.[16] The injections were performed five times a week at approximately 10.00 hours. The animals were killed 48 h after the final administration. Both kidneys and the central lobe of the liver were immediately excised. Half of one kidney and a portion of the liver were used for histological and immunohistochemical analysis, and the rest of the kidney was frozen in liquid nitrogen and stored at −80°C for mutational analyzes.

Monoclonal antibodies. Monoclonal antibody N45.1 recognizing 8-hydroxy-2′-deoxyguanosine (8-OHdG)[32] and monoclonal antibody mAb21 recognizing acrolein-2′-deoxyadenosine adduct (acrolein-dA)[33] were used.

Histological and immunohistochemical analyzes. Kidney specimens were fixed with phosphate-buffered 10% formalin and embedded in paraffin, cut at 3-μm thickness and stained with hematoxylin and eosin staining. For immunohistochemical analyzes, the avidin-biotin complex method with peroxidase was used as described previously.[32,33]

DNA immunoprecipitation and quantitative PCR analysis. To evaluate the relative abundance of Fe-NTA-induced oxidative DNA base modifications (8-OHdG and acrolein-dA) at desired genomic loci, we developed a technique designated as DnaIP (DNA immunoprecipitation).[34] More details will be published elsewhere.[35] Briefly, genomic DNA was extracted from each kidney of *gpt* delta transgenic mice with the NaI method (Wako) using argon gas-saturated buffer to avoid further oxidation during the extraction procedures.[36] Twenty μg of genomic DNA was digested with *Hae*III (TakaraBio, Shiga, Japan), and incubated with each antibody (10 μg of N45.1 or 2 μg of mAb21) in 10 mM phosphate-buffered saline, pH 7.4, containing 0.1% bovine serum albumin, for 3 h at 4°C in a 900-μL volume. The mixture was then incubated with 100 μL of Dynabeads M-280 sheep antimouse IgG (Dynal, Oslo, Norway) for another 3 h, washed sequentially with four different buffers (buffer 1: 0.1% sodium deoxycholate, 1% Triton X-100, 1 mM EDTA, 50 mM HEPES-KOH, 140 mM NaCl, pH 7.5; buffer 2: 0.1% sodium deoxycholate, 1% Triton X-100, 1 mM EDTA, 50 mM HEPES-KOH, 500 mM NaCl, pH 7.5; buffer 3: 0.1% sodium deoxycholate, 0.5% Nonidet P-40, 1 mM EDTA, 250 mM LiCl, 10 mM Tris-HCl, pH 8.0; and buffer 4: 1 × TE). Beads-bound DNA was recovered by incubating the beads with 80 μL of elution buffer (10 mM EDTA, 1% SDS, 50 mM Tris-HCl, pH 8.0) at 65°C for 10 min, and was amplified twice by PCR after ligation to an adaptor (sense, 5′-OH-GGAATTCGGCGGCCGCGGATCC-3′; antisense, 5′-GGATCC-GCGGCCGCCG-3′; sense oligonucleotides were used as primers for amplification), treated with exonuclease I (TakaraBio) and purified with phenol-chloroform extraction. The purified products were subjected to Real-Time PCR (7300 Real Time PCR System, Applied Biosystems, Tokyo) using Platinum SYBR Green qPCR SuperMix UDG (Invitrogen, Tokyo). The primer pairs used were as follows: *gpt*, forward-5′-GCCTTCTGAACAATGGAAAGG-3′, reverse-5′-CGTGATCGTAGCTGGAAATAC-3′ (125 bp); β-*actin*, forward-5′-TCCAACAAACCAAGAGAAATCC-3′, reverse-5′-CGACCTCTGAAACAATTCTGGT-3′ (108 bp); C15-49–5 (chromosome 15, extrageneic region), forward-5′-TGGTACCTGAGT-AAGGCAAGGT-3′, reverse-5′-CCCACTTGTGATTGCTTTCTTC-3′ (107 bp); C16-47–2 (chromosome 16, extrageneic region): forward-5′-CACACACACATGCACACTGTACT-3′, reverse-5′-GCATTTCTCCTCACATTCAGACT-3′ (114 bp); C16-47–5 (chromosome 16, extrageneic region): forward-5′-CCAATTGG-AGCTAACAGAAACC-3′, reverse-5-AGCTGGTCAACTGCC-TACTCTC-3′ (125 bp). These three extrageneic areas were selected based on our observations that chromosome 15 is peripherally located and chromosome 16 is centrally located in the murine renal tubular cells at interphase.[35]

***In vitro* phage packaging.** Genomic DNAs were extracted with the phenol-chloroform extraction protocol.[37] Trangenic *lambda EG10* DNA was rescued from the host genomic DNA using Transpack Packaging Extract (Stratagene, La Jolla, CA) according to the manufacturer's instructions.[30]

Mutation analysis. The 6-TG mutation assay protocol has been described elsewhere.[38–40] Briefly, rescued phage was infected into YG 6020 *E. coli* expressing Cre enzyme, converted into a plasmid carrying the *Cm-resistance* gene and *gpt* gene, and poured on plates containing chloramphenicol (Cm) with or without 6-TG. The positive clones carrying the mutant *gpt* gene were obtained from 6-TG selection plates by incubating at 37°C for 96 h. Selected clones were confirmed again by plating on 6-TG selection plates. The whole *gpt* sequence was amplified from positive clones and identified by sequencing with an ABI PRIZM 377 sequencer. The primers used for amplifying and sequencing were as follows: forward-5′-GCGCAACCTATTTTCCCCTCGA-3′ and reverse-5′-TGGAAACTATTGTAACCCGCCTG-3′. The same primer pair was used for direct sequencing.[41] *E. coli* XL1-Blue MRA and XL1-Blue MRA (P2) were infected with the packaged phage. *E. coli* XL1-Blue MRA was poured onto NZY plates and XL1-Blue MRA (P2) was poured onto I-trypticase agar plates. Plaques that grew on the XL1-Blue MRA (P2) plates were selected and further confirmed with *E. coli* XL1-Blue MRA, *E. coli* WL95 (P2) and XL1-Blue MRA (P2). Positive plaques were recovered and used for determining the deletion position of the *red/gam* gene. Clones or plaques were counted for determining mutant frequencies (MFs). MFs were calculated by using established methods as described previously.[30,42,43]

Hybridization assay and PCR analysis for Spi⁻ mutant analysis. A protocol for Southern blot analysis for Spi⁻ (sensitive to P2 interference) mutants has been established.[43] Seventeen oligomers located within ~14 kb flanking sequence of the *red/gam* gene were used as probes for identifying the deletion junctions. These oligomers were named 18874R, 19258R, 20341R, 21328R, 22556R, 22869R, 23921R, 24858R, 25389F, 26704F, 27096F, 28165F, 29290F, 30104F, 31070F, 31879F and 32890F according to their position as described.[43] The oligomers were spotted onto Hybond™-N⁺ membrane (Amersham) and cross-linked with UV. PCR products, which were amplified by primer 18874R and 32890F using positive individual plaques as templates, were labeled with (α-^{32}P) dCTP using the Megaprime DNA labeling System (Amersham). The membranes were incubated with labeled PCR products at 50°C overnight, washed three times and exposed to BioMax film (Kodak, New York, NY). Deleted regions were located within those oligomers whose signals could not be observed on the film. The nearest primers were selected for PCR amplification and the PCR products were subjected to sequencing to determine the exact deletion junction.

doi: 10.1111/j.1349-7006.2006.00301.x

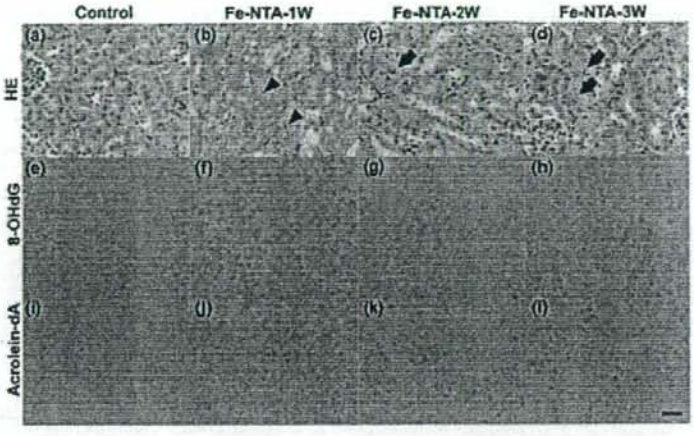

Fig. 1. Immunohistochemical analysis of 8-hydroxy-2'-deoxyguanosine (8-OHdG) and acrolein-modified 2'-deoxyadenosine after repeated administration of ferric nitrilotriacetate (Fe-NTA). (a–d) Hematoxylin and eosin (HE) staining. Regenerative proximal tubular cells were prominent at the first week, together with some necrotic cells (b, ▶). At the second and third week, necrotic cells were no longer observed but increasing numbers of karyomegalic cells (c and d, ▶) appeared. (e–h) Immunohistochemistry of 8-OHdG. Nuclear immunopositivity was observed after Fe-NTA administration, with the highest level after repeated administration for 1 week (f). (i–l) Immunohistochemistry of acrolein-dA. Nuclear immunopositivity was observed after Fe-NTA administration with that of repeated administration of 1 week the highest level (j). Refer to the Materials and Methods section for details (bar in l, 50 μm).

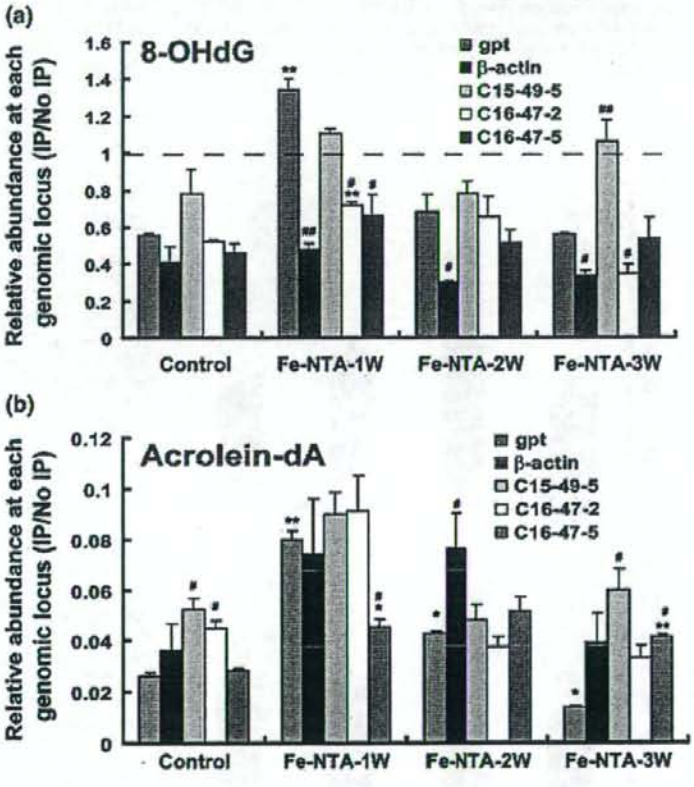

Fig. 2. Real-time polymerase chain reaction (RT-PCR) analysis after DNA immunoprecipitation for quantitation of oxidatively modified DNA bases at specific genomic loci. Renal genomic DNA was digested with *Hae*III and subjected to immunoprecipitation (IP) with specific monoclonal antibodies against 8-hydroxy-2'-deoxyguanosine (8-OHdG) and acrolein-dA. The recovered DNA fragments were amplified after ligation to an adapter and were used as substrates for RT-PCR analyses of *gpt*, β-*actin* and three extrageneic regions at chromosome 15 or 16. Data are shown as relative abundance of PCR products amplified from recovered genomic DNA by IP per those amplified from the original genomic DNA in the same amounts. (a) 8-OHdG. (b) Acrolein-dA. Refer to the Materials and Methods section for details ($N = 3$, means ± SEM; $^{*}P < 0.05$, $^{**}P < 0.01$ versus untreated control kidney at the same genomic region; $^{\#}P < 0.05$, $^{\#\#}P < 0.01$ versus *gpt* locus data of the same treatment group).

Statistical analysis. Statistical analyzes were performed with an unpaired *t*-test, which was modified for unequal variances when necessary.

Results

Renal histology after repeated Fe-NTA administration. As shown in Fig. 1a, no significant histological changes were observed in the kidney of the untreated control group. In contrast, pyknotic nuclei of proximal tubular cells revealing degeneration were scattered in the kidney of mice after 1 week of Fe-NTA treatment (Fig. 1b). Degenerative tubular cells were no longer observed there after 2 or 3 weeks of repeated Fe-NTA treatment, but atypical regenerative cells with a large nucleus containing prominent nucleoli were gradually increased (Fig. 1c,d). In either case, histological evaluation of the liver showed no apparent alterations (data not shown).

Oxidative DNA damage induced by repeated Fe-NTA administration. Two major oxidative DNA base modifications, 8-OHdG and acrolein-dA, were evaluated with immunohistochemistry and DnaIP. Intense diffuse nuclear immunostaining of 8-OHdG and acrolein-dA was prominent in the renal proximal tubules after repeated Fe-NTA administration for 1 week, and gradually decreased thereafter (Fig. 1e–l). To assess whether these oxidative modifications were increased in the *gpt* gene locus, quantitative PCR analysis after DnaIP was performed. The *gpt* reporter gene locus after 1 week of repeated Fe-NTA administration showed higher amounts of 8-OHdG and acrolein-dA than that in the untreated control group. Similar patterns were also observed in the other loci examined, but the *gpt* locus was the most sensitive at the first week (Fig. 2), consistently with the immunohistochemical data (Fig. 1e–l).

Fe-NTA-induced mutant frequencies in *gpt* and *red/gam* genes. We then investigated the reporter genes, *gpt* and *red/gam*, to analyze Fe-NTA-induced mutations using the 6-TG and Spi$^-$ selection systems. In both 6-TG and Spi$^-$ selections, the mutation frequencies were significantly increased (2.44-fold increase in 6-TG selection and 1.72-fold increase in Spi$^-$ selection) after 1 week of repeated Fe-NTA administration (Fig. 3), which was consistent with the results of immunohistochemistry (Fig. 1e–l) and DnaIP (Fig. 2).

Fe-NTA-induced *gpt* gene mutations. To further characterize the exact *gpt* mutations caused by Fe-NTA, 79 mutant clones, in which 69 clones were from Fe-NTA-treated mice and 10 from untreated control mice, were analyzed (Table 1 and Fig. 4). Among the mutations induced by Fe-NTA, 75.4% (52/69) were single base substitutions, of which more than half (32/52 = 61.5%) occurred at G:C base pairs, whereas GC content of *gpt* gene was 46.6%. Among the Fe-NTA-induced substitutions, 40.4% (21/52) were transitions, including G:C to A:T (13/21) and A:T to G:C (8/21), whereas the rest of substitutions (31/52 = 59.6%) were transversions, including G:C to T:A (5/31), G:C to C:G (14/31), A:T to T:A (4/31) and A:T to C:G (8/31) (Table 1). In addition, 17.4% (12/69) of mutant clones were identified as carrying single- or mutiple-base deletions. Among them, 9/12 were single-base deletions, which occurred preferentially at repeated sequences (Table 1 and Fig. 4). Four insertional mutations and one tandem base substitution were also observed. In contrast, analyses of a total of 10 clones from the untreated control kidney showed that 8/10 were single-base substitutions with a single-base deletion and an insertion. In either case, complex mutations were not observed. Therefore, the results indicated that Fe-NTA-induced *gpt* gene mutation preferentially consisted of single-base substitutions occurring at G:C base pairs, in which transversions were more frequent than transitions (Table 1).

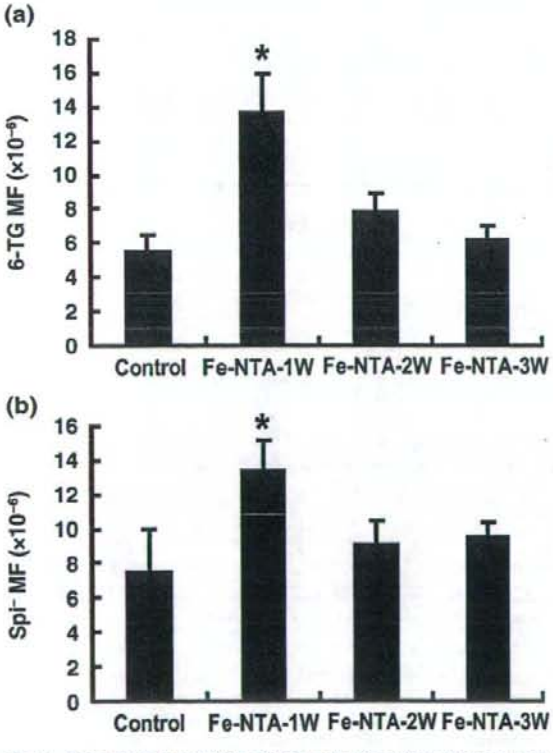

Fig. 3. Mutant frequency (MF) of 6-TG and Spi$^-$ seletion. 6-TG selection was used for the detection of base substitutions in the *gpt* gene; Spi$^-$ selection was used for the detection of large-size deletions. Refer to the Materials and Methods section for details. ($N = 3$, means ± SEM; $^*P < 0.05$, $^{**}P < 0.01$ *versus* untreated control kidney).

Fe-NTA-induced Spi$^-$ mutations. To characterize the Spi$^-$ mutations induced by Fe-NTA, 93 positive plaques obtained from either the kidneys of Fe-NTA-treated mice or untreated control mice were screened by Southern blot analysis followed by sequencing that resulted in the confirmation of 21 large-size deletions (Fig. 5a). Large-size deletions were at first roughly positioned on ~14 kb of sequence spanning the *red/gam* gene by the use of 17 different oligomers as probes. We detected signals for all the 17 oligomer probes in the blot with hybridization to the wild-type *lambda EG 10* (Fig. 5b i). Signals for certain oligomers were absent with Spi$^-$ mutant plaques containing large-size deletions, as shown in Fig. 5(b ii–iv). Most of the large deletions induced by Fe-NTA were more than 1 kb in size (Class I mutation,[31] (Fig. 5a). Furthermore, the majority of them (70.6%) had short homologous sequences of 1–6 bp at the junctions (Class I-A), and in many cases showed three bp or longer running sequences at the junction or its vicinity. Five cases of large-size deletions were accompanied by simultaneous single-base deletion in the *red/gam* gene (Fig. 5a).

Discussion

In the present experiments we have for the first time studied the mutation spectrum of the Fenton reaction-based renal tubular damage in a model of oxidative stress-induced carcinogenesis mediated by Fe-NTA. We intentionally avoided the acute periods for evaluation because of the abundance of necrosis and apoptosis,[20,44] and thus used the subacute phase when the majority of the tubular cells become resistant to oxidative stress with rare cell death present (Fig. 1b–d), though mutation spectrum might be slightly different between the acute and subacute phases. The accumulation of two different kinds of oxidative DNA base modifications, 8-OHdG and acrolein-dA, was most evident with immunohistochemistry after the first week of repeated administration of Fe-NTA and gradually decreased thereafter (Fig. 1e–l). This is probably due to the activation in the cellular metabolic pathways for those either suppressing the Fenton reaction or promoting DNA repair mechanisms. It is also possible that cellular selective processes worked to remove heavily damaged cells.

Gpt delta transgenic mice are an established model for analyzing mutations *in vivo*, and have been used to analyze several possible mutagens.[31] Here we have used a technique designated as DnaIP to evaluate the relative abundance of the two DNA base modifications at the *gpt* loci. Approximately 80 copies of the

doi: 10.1111/j.1349-7006.2006.00301.x

Table 1. Spectrum of Fe-NTA-induced mutations in the kidney of *gpt* delta transgenic mice

Mutation type	Nucleotide position	Sequence change	Amino acid change	Fe-NTA 1w	Fe-NTA 2w	Fe-NTA 3w	Control
Transition					30.4%		50.0%
G:C–A:T	27	G–A	Trp–STOP	1			
	39	G–A	Gln–Gln				1
	64	C–T	Arg–STOP	1			1
	110	G–A	Arg–His	5			1
	113	G–A	Arg–His				1
	116	G–A	Arg–Arg			1	
	128	G–A	Val–Met		1	1	
	287	C–T	Thr–Ile	1			
	356	G–A	Arg–His		1		
	447	C–T	Ile–Ile			1	
A:T–G:C	2	T–C	Met–Thr		1		
	25	T–C	Trp–Ser	1	2		
	188	A–G	Tyr–Cys		1		
	275	A–G	Asp–Gly				1
	307	A–G	Met–Val	1			
	410	A–G	Gln–Arg		1		
	415	T–C	Trp–Arg			1	
Transversion					44.9%		30.0%
G:C–T:A	3	G–T	Ser–Ile		1		
	110	G–T	Arg–His		1		
	115	G–T	Gly–Cys	1			
	189	C–A	Tyr–STOP	1			
	324	C–A	His–Gln				1
	418	G–T	Asp–Try	1			
G:C–C:G	109	C–G	Arg–Gly			1	
	125	C–G	Pro–Arg			1	
	238	G–C	Asp–His			1	
	297	G–C	Ala–Ala	2			
	413	C–G	Pro–Arg	2	1		
	414	G–C	Pro–Pro	2			
	427	G–C	Val–Leu	1		1	
	430	G–C	Val–Leu	2			1
A:T–T:A	52	A–T	Lys–STOP	1			
	66	A–T	Arg–Arg			1	
	179	T–A	Ile–Asn		1	1	
A:T–C:G	94	A–C	Ile–Leu		1		
	133	T–G	Phe–Val		1		
	134	T–G	Gly–STOP		1	1	
	146	A–C	Glu–Ala		1		
	286	A–C	Thr–Pro	1		1	
	315	A–C	Pro–Pro	1			
	375	T–G	Tyr–STOP				1
Deletions					17.4%		10.0%
1 base pair	8–12	AAAAA–AAAA		1	3	1	1
	88–90	AAAGG–AAGG				1	
	423–425	GGGCG–GGCG		1			
	430	TCGTA–TCTA				1	
	437	CGTCC–CGCC				1	
>2 base pairs	156–162	ATTCGTCATGT–ATCG			1		
	170–171	TACCG–TAG			1		
	252–253	TTCATC–TTTC			1		
Insertions					5.7%		10.0%
	74–75	CCTT–CCAATT				1	
	122–123	GTAC–GTTAC		1			
	310–311	ATCC–ATTCC			1	1	
	440–441	CCGC–CCCGC					1
Other					1.4%		0.0%
CC–AG	124–125	TACCGG–TAAGGG			1		

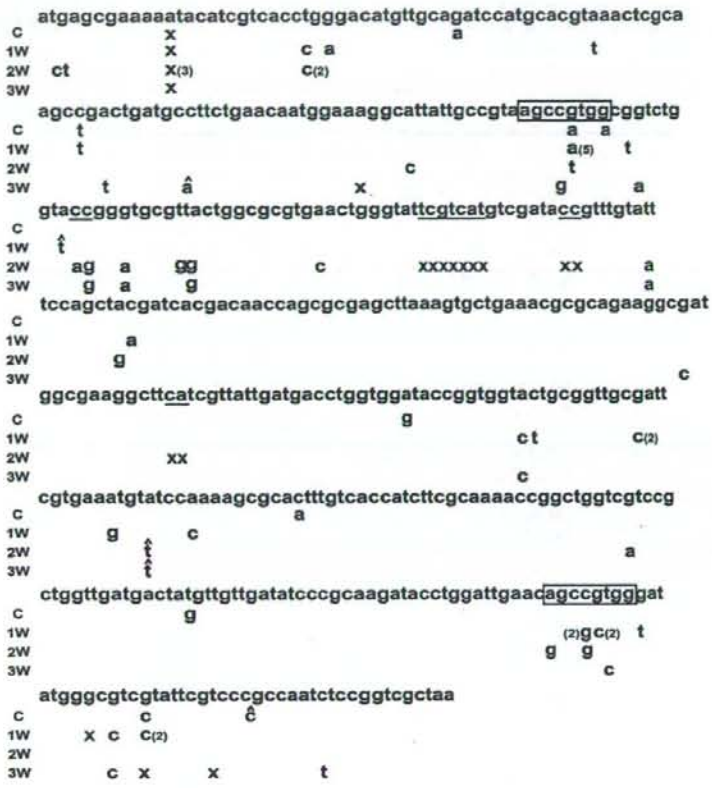

Fig. 4. The position of point mutations in the *gpt* gene. Refer to the Materials and Methods section for details (x, deletion; ^, insertion; underline, more than one base pair deletion within the same case; the number in parenthesis indicates the multiplicity of the same mutation. Square (in one letter), mutation-prone area with the same sequence.

transgenes are included per haploid genome in the *gpt* delta transgenic mice.[30] Among genomic loci examined, including β-actin and three extrageneic regions, the *gpt* loci showed the highest level of 8-OHdG and acrolein-dA after one week of repeated Fe-NTA administration (Fig. 2). This consistency with the immunohistochemical data demonstrates that the transgenic *gpt* loci are indeed vulnerable and suitable for mutational analyzes. We believe that the high copy number of the *gpt* gene contained in these mice is at least partially responsible for this reliable sensitivity. In contrast to the findings at one week, certain extrageneic loci showed significantly higher levels of DNA base modifications than the *gpt* gene locus at other time points, suggesting that further studies would be necessary to elucidate the principles governing the distribution of oxidative DNA base modifications over the whole genome.[35,45]

Mutation frequencies both for the 6-TG selection and Spi$^-$ selection also were the highest at the first week of repeated Fe-NTA administration (Fig. 3). This confirms the usefulness of 8-OHdG and acrolein-dA, which were detected both by immunohistochemistry and DnaIP, as reliable markers of mutation. In 22.7% of the Spi$^-$ plaques after Fe-NTA treatment, large-size deletions (>1 kb) were observed and most of them were class I-A mutants (Fig. 5). This preference for large-size deletions with short homologous sequences at the junctions might be a prominent feature of the results obtained in this renal carcinogenesis model in that the patterns of Spi$^-$ mutations are similar to that of the untreated colon.[31] With γ-rays, shorter deletions than 1 kb are prominent; with UVB and MMC, large-size deletions with or without short homologous sequences at the junctions are more frequently observed (>40%); whereas with PhIP and APNH, large-size deletions were rare.[31]

In the Fe-NTA-induced renal cell carcinoma of rats, homozygous deletion of the *p16^{INK4A}* tumor suppressor gene was frequently observed,[21] and the allelic loss of this locus was observed at a high frequency one to three weeks after the repeated administration of Fe-NTA in rats.[22] We believe that the iron-mediated Fenton reaction is mainly responsible for this characteristic deletion. Short deletions were also increased after Fe-NTA administration (Table 1). Probably, the free radical reaction associated with iron is distinct from the reactions associated with other agents studied so far in the *gpt* lambda transgenic mice in that this is a universal reaction, though exaggerated through iron overload, involving the generation of hydroxyl radical and lipid peroxidation products. This kind of reaction is always taking place in the body under conditions of normal metabolism associated with oxygen consumption and, though it results in only minor consequences under physiological conditions, can be a driving force of carcinogenesis.

The mutation spectrum detected in the *gpt* gene was also quite distinctive. G:C pairs were the preferred bases for mutation, and especially G:C to C:G transversion-type mutation was characteristic (Fig. 4 and Table 1). This type of mutation was observed in PhIP and MMC as a minor type, but has not been reported as a major type of mutation (Table 2). We observed a low incidence of G:C to T:A transversion-type mutation that results from

doi: 10.1111/j.1349-7006.2006.00301.x

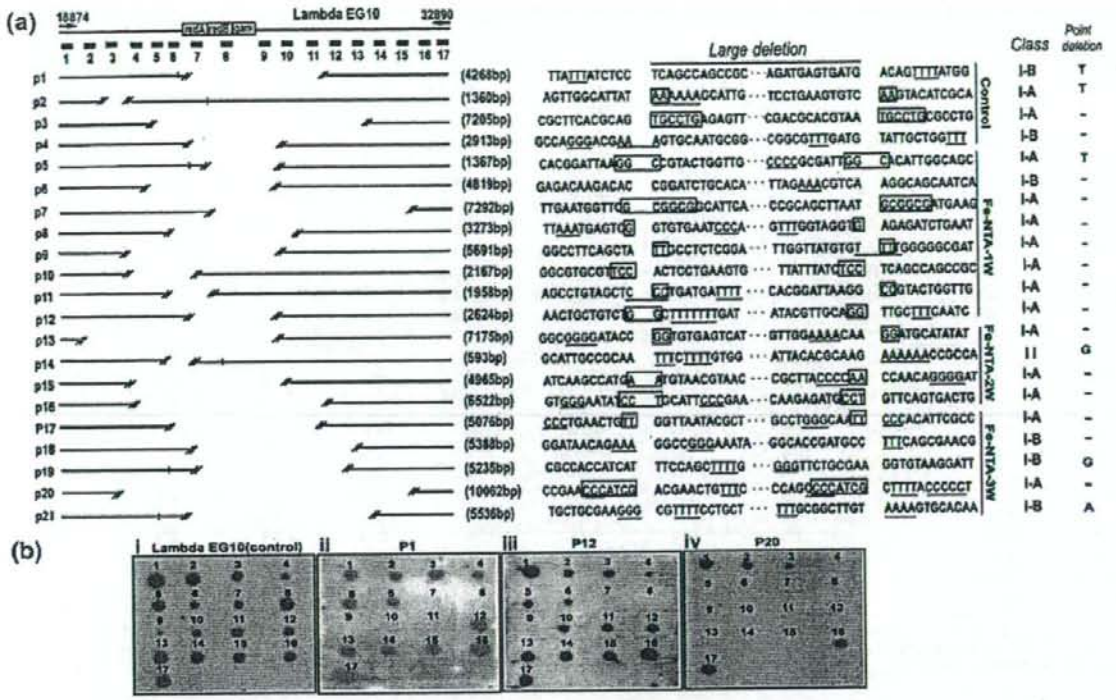

Fig. 5. Size and position of large-size deletions after Spi⁻ selection with each junctional sequence. (a) Summary of the strategy and the observed deletions. P1–P4, untreated control; P5–P21, ferric nitrilotriacetate (Fe-NTA)-induced deletions. Blank areas between two double-dash lines indicate large-size deletions; short longitudinal lines indicate accompanying 1-base deletion; □, short homologous sequence; underline, short run more than 3 bp. Classification of the deletion type was done as described.[31] (b) Representative results of Southern blotting analysis for screening the deleted positions. Arabic numerals (1–17) indicate the probes used as described in the Materials and Methods section and P1, P12 and P20 correspond to the a section.

8-OHdG formation.[46,47] This may be explained by the fact that this mutagenic process is strongly inhibited by a DNA repair enzyme, Mutyh.[48] Here we may propose a mechanism in which certain oxidative modification to guanine/cytosine may cause abnormal pairing with the same corresponding base. Recently, it was reported that formamidopyrimidine (FaPy)-guanine, another oxidative DNA base modification,[49,50] would not be responsible for this type of mutation.[51] We suspect that 5,6-dihydroxyuracil and 5-hydroxycytosine which are increased in this model[17] or other aldehyde-modified bases than acrolein-dA are among the possible candidates.

When we reviewed the spectrum of point mutation observed in the *p53*, *tsc2*, *p15*, *p16 and tbp-2* tumor suppressor genes of Fe-NTA-induced rat renal carcinoma, we observed no G:C to C:G transversions, but G:C to T:A (*p53*, *tbp-2*),[16,24] T:A to C:G (*tsc2*), G:C to A:T (*p15 and p16*, *tbp-2*),[21] A:T to T:A (*tbp-2*)[24] and one nucleotide insertion/deletion at repeat sequences (*p16*, *tbp-2*)[21,24] were observed despite the limited available data. There are at least several possibilities to explain this: (i) we have not yet identified the target genes with G:C to C:G mutations; (ii) there are some species-differences between mice and rats; (iii) this mutation spectrum detected in this *gpt* transgenic system is largely reflected in non-geneic genome areas; and (iv) the last possibilities are that G:C to C:G mutations are preferentially repaired by mismatch repair enzyme(s) in non-transgene areas or abundant mutations of this kind lead to lethal effects, affecting fundamental transcriptional activity in the expressed genes. Regarding species differences, another study using the *gpt* delta transgenic rat[52] would answer the question. The data obtained with DnaIP is of note in that 8-OHdG and acrolein-dA were increased in some non-geneic regions after three weeks of repeated administration of Fe-NTA, warranting further studies.

In conclusion, we used the *gpt* delta transgenic mice to evaluate the mutation spectrum of the Fenton reaction-based oxidative renal tubular injury, and found that the major mutations consist of large-size deletions with short homologous sequences at the junctions and transversion-type point mutations at G:C base pairs. The mutant frequency was the highest at the first week of repeated Fe-NTA administration, as shown by the immunohistochemistry of 8-OHdG and acrolein-dA as well as the presence of these two modified bases at the *gpt* loci, indicating that this early stage is one of the critical periods in this Fenton reaction-induced carcinogenesis.

Acknowledgments

This work was supported in part by a Grant-in-Aid from the Ministry of Education, Culture, Sports, Science and Technology of Japan, a Grant-in-Aid for Cancer Research from the Ministry of Health, Labour and Welfare of Japan, and a grant of Long-range Research Initiative (LRI) by Japan Chemical Industry Association (JCIA).

Table 2. Comparison of mutations induced by various mutagens in *gpt* delta transgenic mice

Target	Kidney[†]				Bone marrow[38]		Colon[39]	
	Control (MF = 1.0)	Fe-NTA-1 W (MF = 2.4)	Fe-NTA-2 W (MF = 1.4)	Fe-NTA-3 W (MF = 1.1)	Control (MF = 1.0)	PhIP (MF = 10.9)	Control (MF = 1.0)	ENU (MF = 3.2)
G:C–A:T	40%	28.6% (1.72)	8.7% (0.30)	16.7% (0.46)	43.1%	14.1%	26.9%	28.3%
A:T–G:C	10%	7.1% (1.70)	21.7% (3.04)	5.6% (0.62)	11.1%	0.0%	3.8%	20.0%
G:C–T:A	10%	10.7% (2.57)	8.7% (1.21)	0% (0.00)	26.4%	52.5%	11.5%	15.0%
G:C–C:G	10%	32.1% (7.70)	4.3% (0.60)	22.2% (2.44)	0.0%	13.1%	7.7%	0.0%
A:T–T:A	0%	3.6% (∞)	4.3% (∞)	11.1% (∞)	5.6%	1.0%	3.8%	28.3%
A:T–C:G	10%	7.1% (1.70)	17.4% (2.44)	11.1% (0.62)	4.2%	0.0%	0.0%	5.0%
Deletion	10%	7.1% (1.70)	26.1% (3.65)	22.2% (2.44)	4.2%	15.1%	38.5%	3.3%
Insertion	10%	3.6% (0.86)	4.3% (0.60)	11.1% (1.22)	5.6%	1.0%	7.7%	0.0%
Others	0%	0.0% (NA)	4.3% (∞)	0.0% (NA)	0.0%	3.0%	0.0%	0.0%

Target	Bone marrow[41]		Liver[53]		Liver[54]		Epidermis[55]		Liver[56]	
	Control (MF = 1.0)	MCC (MF = 2.9)	Control (MF = 1.0)	APNH (MF = 10.3)	Control (MF = 1.0)	γ-ray (MF = 3.2)	Control (MF = 1.0)	UVB (MF = 7.7)	Control (MF = 1.0)	MeIQx (MF = 8.6)
G:C–A:T	24.1%	13.3%	41%	23%	27%	20%	64%	87%	43%	16%
A:T–G:C	3.4%	6.7%	10%	1%	15%	0%	0%	3%	8%	0%
G:C–T:A	31.0%	26.7%	14%	51%	12%	25%	9%	0%	10%	54%
G:C–C:G	10.3%	6.7%	2%	1%	4%	0%	0%	1%	4%	5%
A:T–T:A	6.9%	3.3%	8%	0%	4%	0%	9%	4%	8%	3%
A:T–C:G	10.3%	3.3%	4%	0%	23%	10%	10%	0%	2%	0%
Deletion	13.8%	6.7%	18%	16%	12%	35%	18%	0%	12%	16%
Insertion	0.0%	0.0%	2%	0%	4%	10%	0%	0%	2%	0%
Others	0.0%	33.3%	2%	7%	0%	0%	0%	5%	11%	6%

[†]present study. The number in parenthesis is the relative mutation frequency in comparison to the untreated control. MF, mutation frequency; NA, not applied; W, week(s); Fe-NTA, ferric nitrilotriacetate; PhIP, 2-amino-1-methyl-6-phenylimidazo [4,5-b]pyridine; ENU, ethylnitrosourea; MMC, mitomycin C; APNH, aminophenylnorharman; UVB, ultraviolet B; MeIQx, 2-amino-3,8-dimethylimidazo[4,5-f]quinoxaline.

References

1 Halliwell B, Gutteridge JMC. *Free radicals in biology and medicine*. Oxford: Clarendon Press, 1999.
2 Iuchi K, Ichimiya A, Akashi A *et al.* Non-Hodgkin's lymphoma of the pleural cavity developing from long-standing pyothorax. *Cancer* 1987; **60**: 1771–5.
3 Gilmour P, Brown D, Beswick P, MacNee W, Rahman I, Donaldson K. Free radical activity of industrial fibers: role of iron in oxidative stress and activation of transcription factors. *Environ Health Perspect* 1997; **105** (Suppl 5): 1313–17.
4 Hodgson J, Darnton A. The quantitative risks of mesothelioma and lung cancer in relation to asbestos exposure. *Ann Occup Hyg* 2000; **44**: 565–601.
5 Uemura N, Okamoto S, Yamamoto S *et al. Helicobacter pylori* infection and the development of gastric cancer. *N Engl J Med* 2001; **345**: 784–9.
6 Naito Y, Yoshikawa T. Carcinogenesis and chemoprevention in gastric cancer associated with *helicobacter pylori* infection: role of oxidants and antioxidants. *J Clin Biochem Nutr* 2005; **36**: 37–49.
7 Collins R, Feldman M, Fordtran J. Colon cancer, dysplasia, and surveillance in patients with ulcerative colitis. A critical review. *N Engl J Med* 1987; **316**: 1654–8.
8 Eaden J, Abrams K, Mayberry J. The risk of colorectal cancer in ulcerative colitis: a meta-analysis. *Gut* 2001; **48**: 526–35.
9 Toyokuni S. Iron-induced carcinogenesis: the role of redox regulation. *Free Radic Biol Med* 1996; **20**: 553–66.
10 Elmberg M, Hultcrantz R, Ekbom A *et al.* Cancer risk in patients with hereditary hemochromatosis and in their first-degree relatives. *Gastroenterology* 2003; **125**: 1733–41.
11 Grodstein F, Speizer F, Hunter D. A prospective study of incident squamous cell carcinoma of the skin in the nurses' health study. *J Natl Cancer Inst* 1995; **87**: 1061–6.
12 Nishigori C, Hattori Y, Toyokuni S. Role of reactive oxygen species in skin carcinogenesis. *Antioxid Redox Signal* 2004; **6**: 561–70.
13 Preston D, Kusumi S, Tomonaga M *et al.* Cancer incidence in atomic bomb survivors. Part III. Leukemia, lymphoma and multiple myeloma, 1950–87. *Radiat Res* 1994; **137**: S68–97.
14 Li JL, Okada S, Hamazaki S, Ebina Y, Midorikawa O. Subacute nephrotoxicity and induction of renal cell carcinoma in mice treated with ferric nitrilotriacetate. *Cancer Res* 1987; **47**: 1867–9.
15 Ebina Y, Okada S, Hamazaki S, Ogino F, Li JL, Midorikawa O. Nephrotoxicity and renal cell carcinoma after use of iron- and aluminum-nitrilotriacetate complexes in rats. *J Natl Cancer Inst* 1986; **76**: 107–13.
16 Nishiyama Y, Suwa H, Okamoto K, Fukumoto M, Hiai H, Toyokuni S. Low incidence of point mutations in *H-*, *K-* and *N-ras* oncogenes and *p53* tumor suppressor gene in renal cell carcinoma and peritoneal mesothelioma of Wistar rats induced by ferric nitrilotriacetate. *Jpn J Cancer Res* 1995; **86**: 1150–8.
17 Toyokuni S, Mori T, Dizdaroglu M. DNA base modifications in renal chromatin of Wistar rats treated with a renal carcinogen, ferric nitrilotriacetate. *Int J Cancer* 1994; **57**: 123–8.
18 Toyokuni S, Uchida K, Okamoto K, Hattori-Nakakuki Y, Hiai H, Stadtman ER. Formation of 4-hydroxy-2-nonenal-modified proteins in the renal proximal tubules of rats treated with a renal carcinogen, ferric nitrilotriacetate. *Proc Natl Acad Sci USA* 1994; **91**: 2616–20.
19 Toyokuni S, Luo XP, Tanaka T, Uchida K, Hiai H, Lehotay DC. Induction of a wide range of C_{2-13} aldehydes and C_{7-13} acyloins in the kidney of Wistar rats after treatment with a renal carcinogen, ferric nitrilotriacetate. *Free Radic Biol Med* 1997; **22**: 1019–27.
20 Zhang D, Okada S, Yu Y, Zheng P, Yamaguchi R, Kasai H. Vitamin E inhibits apoptosis, DNA modification, and cancer incidence induced by iron-mediated peroxidation in Wistar rat kidney. *Cancer Res* 1997; **57**: 2410–14.
21 Tanaka T, Iwasa Y, Kondo S, Hiai H, Toyokuni S. High incidence of allelic loss on chromosome 5 and inactivation of $p15^{INK4B}$ and $p16^{INK4A}$ tumor suppressor genes in oxystress-induced renal cell carcinoma of rats. *Oncogene* 1999; **18**: 3793–7.
22 Hiroyasu M, Ozeki M, Kohda H *et al.* Specific allelic loss of $p16^{INK4A}$ tumor suppressor gene after weeks of iron-mediated oxidative damage during rat renal carcinogenesis. *Am J Pathol* 2002; **160**: 419–24.
23 Tanaka T, Akatsuka S, Ozeki M, Shirase T, Hiai H, Toyokuni S. Redox regulation of annexin 2 and its implications for oxidative stess-induced renal carcinogenesis and metastasis. *Oncogene* 2004; **23**: 3980–9.
24 Dutta KKN, Ishinaka Y, Masutani H *et al.* Thioredoxin-binding protein-2 is a target gene in oxidative stress-induced renal carcinogenesis. *Lab Invest* 2005; **85**: 798–807.
25 Nakatsuka S, Tanaka H, Namba M. Mutagenic effects of ferric nitrilotriacetate (Fe-NTA) on V79 Chinese hamster cells and its inhibitory effects on cell-cell communication. *Carcinogenesis* 1990; **11**: 257–60.

doi: 10.1111/j.1349-7006.2006.00301.x

26 Toyokuni S, Sagripanti JL, Hitchins VM. Cytotoxic and mutagenic effects of ferric nitrilotriacetate on L5178Y mouse lymphoma cells. *Cancer Lett* 1995; **88**: 157–62.
27 Gossen J, de Leeuw W, Tan C *et al*. Efficient rescue of integrated shuttle vectors from transgenic mice: a model for studying mutations in vivo. *Proc Natl Acad Sci USA* 1989; **86**: 7971–5.
28 Kohler S, Provost G, Fieck A *et al*. Spectra of spontaneous and mutagen-induced mutations in the *lacI* gene in transgenic mice. *Proc Natl Acad Sci USA* 1991; **88**: 7958–62.
29 Gondo Y, Shioyama Y, Nakao K, Katsuki M. A novel positive detection system of in vivo mutations in *rpsL* (*strA*) transgenic mice. *Mutat Res* 1996; **360**: 1–14.
30 Nohmi T, Katoh M, Suzuki H *et al*. A new transgenic mouse mutagenesis test system using Spi⁻ and 6-thioguanine selections. *Environ Mol Mutagen* 1996; **28**: 465–70.
31 Nohmi T, Masumura K. Molecular nature of intrachromosomal deletions and base substitutions induced by environmental mutagens. *Environ Mol Mutagen* 2005; **45**: 150–61.
32 Toyokuni S, Tanaka T, Hattori Y *et al*. Quantitative immunohistochemical determination of 8-hydroxy-2′-deoxyguanosine by a monoclonal antibody N45.1: its application to ferric nitrilotriacetate-induced renal carcinogenesis model. *Lab Invest* 1997; **76**: 365–74.
33 Kawai Y, Furuhata A, Toyokuni S, Aratani Y, Uchida K. Formation of acrolein-derived 2′-deoxyadenosine adduct in an iron-induced carcinogenesis model. *J Biol Chem* 2003; **278**: 50 346–54.
34 Toyokuni S, Akatsuka S, Aung TT, Dutta KK. Free radical-induced carcinogenesis: target genes and fragile genome sites. *Free Radic Res* 2005; **39** (Suppl 1): S30.
35 Akatsuka S, Aung TT, Dutta KK *et al*. Contrasting genome-wide distribution of 8-hydroxyguanine and acrolein-modified adenine during oxidative stress-induced renal carcinogenesis. *Am J Pathol* 2006, in press.
36 Nakae D, Mizumoto Y, Kobayashi E, Noguchi O, Konishi Y. Improved genomic/nuclear DNA extraction for 8-hydroxydeoxyguanosine analysis of small amounts of rat liver tissue. *Cancer Lett* 1995; **97**: 233–9.
37 Ono T, Miyamura Y, Ikehata H *et al*. Spontaneous mutant frequency of *lacZ* gene in spleen of transgenic mouse increases with age. *Mutat Res* 1995; **338**: 183–8.
38 Masumura K, Matsui K, Yamada M *et al*. Mutagenicity of 2-amino-1-methyl-6-phenylimidazo [4,5-b]pyridine (PhIP) in the new *gpt* delta transgenic mouse. *Cancer Lett* 1999; **143**: 241–4.
39 Masumura K, Matsui M, Katoh M *et al*. Spectra of *gpt* mutations in ethylnitrosourea-treated and untreated transgenic mice. *Environ Mol Mutagen* 1999; **34**: 1–8.
40 Nohmi T, Suzuki T, Masumura K. Recent advances in the protocols of transgenic mouse mutation assays. *Mutat Res* 2000; **455**: 191–215.
41 Takeiri A, Mishima M, Tanaka K *et al*. Molecular characterization of mitomycin C-induced large deletions and tandem-base substitutions in the bone marrow of *gpt* delta transgenic mice. *Chem Res Toxicol* 2003; **16**: 171–9.
42 Cariello N, Piegorsch W, Adams W, Skopek T. Computer program for the analysis of mutational spectra: application to *p53* mutations. *Carcinogenesis* 1994; **15**: 2281–5.
43 Shibata A, Masutani M, Kamada N *et al*. Efficient method for mapping and characterizing structures of deletion mutations in *gpt* delta mice using Southern blot analysis with oligo DNA probes. *Environ Mol Mutagen* 2004; **43**: 204–7.
44 Hamazaki S, Okada S, Ebina Y, Midorikawa O. Acute renal failure and glucosuria induced by ferric nitrilotriacetate in rats. *Toxicol Appl Pharmacol* 1985; **77**: 267–74.
45 Toyokuni S, Akatsuka S. What has been learned from the studies of oxidative stress-induced carcinogenesis: proposal of the concept of oxygenomics. *J Clin Biochem Nutr* 2006; **39**: 3–10.
46 Shibutani S, Takeshita M, Grollman AP. Insertion of specific bases during DNA synthesis past the oxidation-damaged base 8-oxodG. *Nature* 1991; **349**: 431–4.
47 Kasai H. Analysis of a form of oxidative DNA damage, 8-hydroxy-2′-deoxyguanosine, as a marker of cellular oxidative stress during carcinogenesis. *Mutat Res* 1997; **387**: 147–63.
48 Nakabeppu Y. Regulation of intracellular localization of human MTH1, OGG1, and MYH proteins for repair of oxidative DNA damage. *Prog Nucl Acid Res Mol Biol* 2001; **68**: 75–94.
49 Steenken S. Purine bases, nucleosides, and nucleotides: aqueous solution redox chemistry and transformation reactions of their radical reactions and e⁻ and. OH adducts. *Chem Rev* 1989; **89**: 503–20.
50 Dizdaroglu M. Chemical determination of free radical-induced damage to DNA. *Free Radic Biol Med* 1991; **10**: 225–42.
51 Ober M, Muller H, Pieck C, Gierlich J, Carell T. Base pairing and replicative processing of the formamidopyrimidine-dG DNA lesion. *J Am Chem Soc* 2005; **127**: 18 143–9.
52 Hayashi H, Kondo H, Masumura K, Shindo Y, Nohmi T. Novel transgenic rat for *in vivo* genotoxicity assays using 6-thioguanine and Spi⁻ selection. *Environ Mol Mutagen* 2003; **41**: 253–9.
53 Masumura K, Totsuka Y, Wakabayashi K, Nohmi T. Potent genotoxicity of aminophenylnorharman, formed from non-mutagenic norharman and aniline, in the liver of *gpt* delta transgenic mouse. *Carcinogenesis* 2003; **24**: 1985–93.
54 Masumura K, Kuniya K, Kurobe T, Fukuoka M, Yatagai F, Nohmi T. Heavy-ion-induced mutations in the *gpt* delta transgenic mouse: comparison of mutation spectra induced by heavy-ion, X-ray, and gamma-ray radiation. *Environ Mol Mutagen* 2002; **40**: 207–15.
55 Horiguchi M, Masumura K, Ikehata H *et al*. UVB-induced *gpt* mutations in the skin of *gpt* delta transgenic mice. *Environ Mol Mutagen* 1999; **34**: 72–9.
56 Masumura K, Horiguchi M, Nishikawa A *et al*. Low dose genotoxicity of 2-amino-3,8-dimethylimidazo[4,5-f]quinoxaline (MeIQx) in *gpt* delta transgenic mice. *Mutat Res* 2003; **541**: 91–102.

Genes and Environment, Vol. 28, No. 3 pp. 84–91 (2006)

Regular article

Chemopreventive Effects of Nobiletin against Genotoxicity Induced by 4-(Methylnitrosamino)-1-(3-pyridyl)-1-butanone (NNK) in the Lung of *gpt* delta Transgenic Mice

Megumi Ikeda[1,2], Ken-ichi Masumura[1], Keiko Matsui[1], Hiroyuki Kohno[3], Keiko Sakuma[2], Takuji Tanaka[3] and Takehiko Nohmi[1,4]

[1]Division of Genetics and Mutagenesis, National Institute of Health Sciences, Tokyo, Japan,
[2]Graduate School of Nutrition and Health Sciences, Kagawa Nutrition University, Saitama, Japan,
[3]Department of Oncologic Pathology, Kanazawa Medical University, Ishikawa, Japan

(Received May 22, 2006; Revised June 8, 2006; Accepted June 15, 2006)

Nobiletin, a major component of citrus polymethoxyflavones, possesses anticancer, antiviral and anti-inflammatory activities. To evaluate the chemopreventive potential against lung cancer induced by cigarette smoke, we examined suppressive effects of nobiletin against genotoxicity induced by 4-(methylnitrosamino)-1-(3-pyridyl)-1-butanone (NNK), the most carcinogenic tobacco-specific nitrosamine, in the lung of *gpt* delta transgenic mice. Male and female *gpt* delta mice were fed nobiletin at a dose of 100 or 500 ppm in diet for seven days and treated with NNK at a dose of 2 mg/mouse/day, i.p. for four consecutive days. Dietary administration of nobiletin continued at the doses during the NNK treatments and in the following period before sacrifice at day 38. NNK treatments enhanced the *gpt* mutant frequency (MF) in the lung 19- and 9-fold, respectively, over the values of untreated female and male mice. Interestingly, nobiletin reduced the NNK-induced MFs by 25–45% in both sexes and the reduction at a dose of 100 ppm in females and 500 ppm in males was statistically significant ($P<0.05$). To further characterize the suppressive effects, we conducted bacterial mutation assay with *Salmonella typhimurium* YG7108 to examine whether nobiletin inhibits S9-mediated genotoxicity of NNK. Nobiletin as well as 8-methoxypsoralen, an inhibitor of CYP2A, reduced the genotoxicity of NNK by more than 50%. These results suggest that nobiletin may be chemopreventive against NNK-induced lung cancer and also that the chemopreventive efficacy may be due to inhibition of certain CYP enzymes involved in the metabolic activation of NNK.

Key words: nobiletin, NNK, chemoprevention, cigarette smoking, *gpt* delta transgenic mice

Introduction

Humans are exposed to a variety of exogenous and endogenous genotoxic agents. Of various hazardous environmental factors, cigarette smoke may be the most causative factor associated with the incidence of human cancer (1). Although cigarette smoke contains more than 4,000 compounds including 40 known human carcinogens, 4-(methylnitrosamino)-1-(3-pyridyl)-1-butanone (nicotine-derived nitrosamino ketone, NNK) is the most carcinogenic tobacco-specific nitrosamine (2,3). NNK is estimated to be present at levels of 17–430 and 390–1,440 ng, respectively, per cigarette in mainstream and sidestream of cigarette smoke (3). NNK induces lung tumors in rats, mice and hamsters and is classified into Class 2B carcinogen (possibly carcinogenic to humans) by International Agency for Research on Cancer (4). NNK is metabolically activated by CYP (P-450) enzymes, and the metabolites generate methylated and pyridyloxobutylated DNA, which can induce G:C-to-A:T and G:C-to-T:A mutations, respectively. O^6-Methylguanine in the lung may be a causative lesion of NNK leading to activation of Ki-*ras* protooncogene, an initiation of tumor development (5,6).

With smoking the major etiological factor for lung cancer, a number of naturally occurring and synthetic chemicals have been proposed as candidates of chemopreventive agents to protect smokers who are unwilling or unable to quit smoking. Examples of the candidates include inhibitors of metabolic activation of NNK, e.g., phenethyl isothiocyanate and curcumins (7–10), enhancers of detoxication enzymes, e.g., prodrugs of L-selenocystein (11), antioxidants, e.g., vitamine E and carotenoids (12,13) and inhibitors of signal transduction downstream from the activated oncogenes, e.g., perillyl alcohol and deguelin (14,15).

Nobiletin (5,6,7,8,3′,4′-hexamethoxyflavone) is a

[4]Correspondence to: Takehiko Nohmi, Division of Genetics and Mutagenesis, National Institute of Health Sciences, 1-18-1, Kamiyoga, Setagaya-ku, Tokyo 158-8501 Japan. Tel: +81-3-3700-9873, Fax: +81-3-3707-6950, E-mail: nohmi@nihs.go.jp

polymethoxyflavone found in *Citrus depressa* Rutaceae, a popular citrus fruit in Okinawa, Japan (16). Interestingly, nobiletin seems to possess anticancer activities by inhibiting critical steps of carcinogenesis, i.e., initiation (13,17), promotion (18,19) and metastasis (16,20,21). In addition, nobiletin inhibits the P-glycoprotein drug efflux transporter, suggesting the ability to reverse multi-drug resistance of tumor cells (22).

To evaluate the chemopreventive efficacy against lung cancer induced by cigarette smoke, we examined suppressive effects of dietary administration of nobiletin in the lung of *gpt* delta mice treated with NNK. In this mouse model, base substitutions such as G:C-to-A:T or G:C-to-T:A can be detected by *gpt* selection. In fact, Miyazaki *et al.* (23) have employed the mice to demonstrate the chemopreventive effects of 8-methoxypsoralen against NNK-induced mouse lung adenoma. Besides *in vivo* genotoxicity assays, we conducted a bacterial mutation assay with *Salmonella typhimurium* YG7108 to examine whether nobiletin inhibits the genotoxicity of NNK in the presence of S9 metabolic activation system. The bacterial strain lacks O^6-methylguanine methyltransferase activity, so that it is highly sensitive to base substitution mutations by NNK and other alkylating agents (24,25). The results suggest that nobiletin clearly suppresses the genotoxicity of NNK *in vivo* and *in vitro*. We discuss the mechanisms underlying the suppressive effects and the possible usage of nobiletin as a chemopreventive agent against lung cancer induced by cigarette smoke.

Material and Methods

Materials: Nobiletin (>99.9% purity) was chemically synthesized according to the method described by Tsukayama *et al.* (26) with slight modifications. Sources of other chemicals used in this study are as follows: NNK, Toronto Research Chemicals (Toronto, Canada); benzo[a]pyrene (BP), Wako Pure Chemicals (Osaka, Japan); 8-methoxypsoralen and *N*-methyl-*N'*-nitro-*N*-nitrosoguanidine (MNNG), Sigma-Aldrich Japan K. K. (Tokyo, Japan). S9 prepared from male Sprague-Dawley rats pretreated with phenobarbital and 5,6-benzoflavone was purchased from Kikkoman Cooperation, Chiba, Japan.

Treatment of *gpt* delta mice: Male and female *gpt* delta C57BL/6J transgenic mice, obtained from Japan SLC, Inc. (Shizuoka, Japan), were maintained in Animal Facility of Kanazawa Medical University, according to the institutional animal care guidelines. The animals were housed in plastic cages with free access to tap water and powdered basal diet CRF-1 (Oriental Yeast, Tokyo, Japan) under controlled conditions of temperature at 23 ± 2°C, humidity of 10% and lighting (12 h light-dark cycle). Twenty female and 25 male *gpt* delta mice were each divided into four experimental and one control groups (Fig. 1). When the mice were 8 weeks of age, they were fed diet supplemented with nobiletin at a concentration of 100 ppm (Group 2) or 500 ppm (Groups 3 and 4) for 38 days. Groups 1 through 3 were treated with a single i.p. injection of NNK dissolved in saline at a dose of 2 mg/mouse/day for four consecutive days from day 7 through day 10. Groups 4 and 5 were treated with saline as vehicle. Mice were sacrificed under ether anesthesia at day 38. The lung was removed, placed immediately in liquid nitrogen, and stored at −80°C until analysis.

DNA Isolation, *in vitro* packaging and *gpt* mutation assay: High-molecular-weight genomic DNA was extracted from the lung using the RecoverEase DNA Isolation Kit (Stratagene, La Jolla, CA). λEG10 phages were rescued using Transpack Packaging Extract (Stratagene, La Jolla, CA). The *gpt* mutation assay was performed according to previously described methods (27,28). *gpt* MFs were calculated by dividing the number of colonies growing on agar plates containing chloramphenicol and 6-thioguanine by the product of the number of colonies growing on plates containing chloramphenicol and the dilution factor.

Bacterial mutation assay: The mutagenicity assay was carried out with a pre-incubation method with modifications (29). Nobiletin or 8-methoxypsoralen was dissolved in DMSO and the solution (50 μL) was mixed with S9 mix (0.5 mL). They were kept on ice for 5 min and mixed with the solution (50 μL) of chemicals, i.e., NNK, BP or MNNG, dissolved in DMSO. Then, they were mixed with overnight culture (0.1 mL) and incubated for 20 min at 37°C. When the mutagenicity of MNNG was assayed, 1/15M phosphate buffer pH7.4 (0.5 mL) was added instead of S9 mix. The reaction mixture containing bacteria, nobiletin (or 8-methoxypsoralen) and the chemical with or without S9 mix was poured onto agar plates with soft agar and incubated for two days at 37°C. Each chemical was assayed with 6–8 doses on triplicate or duplicate plates. Tester strains for the mutation assays were *S. typhimurium* YG7108 for NNK and MNNG, and *S. typhimurium* YG5161 (30) for BP. Relevant genotypes of the strains are as follows: YG7108 (24,25) as *S. typhimurium* TA1535 but is Δada_{ST} Δogt_{ST}; YG5161 (30) as *S. typhimurium* TA1538 harboring plasmid pYG768 carrying the *dinB* gene of *Escherichia coli*.

Statistical analysis: All data are expressed as mean ± standard deviations. Differences between groups were tested for statistical significance using a Student's *t*-test. A *P* value less than 0.05 denoted the presence of a statistically significant difference.

Results

Dietary administration of nobiletin suppresses mutations induced by NNK in the lung of *gpt* delta mice: To examine the suppressive effects of nobiletin against genotoxicity induced by NNK, female and male *gpt* delta mice were fed nobiletin in diet at a dose of 100 or 500 ppm for a week and treated with NNK (Fig. 1). Dietary administration of nobiletin continued during the NNK treatments and in the following period before sacrifice at day 38. NNK treatments enhanced *gpt* MF in the lung 19 times in females and 9 times in males over the control levels (Tables 1 and 2). Since the MFs ($\times 10^{-6}$) of untreated controls were similar between females and males (3.0 ± 1.3 versus 3.1 ± 2.0), NNK-induced MF was higher in females (58.1 ± 16.7) than in males (26.5 ± 11.8). Nobiletin itself was non-genotoxic (Group 4). Nobiletin appeared to reduce the MFs in both sexes. In females, the dietary administration of nobiletin at 100 and 500 ppm (Groups 2 and 3) reduced the NNK-induced MF by 34 and 32%, respectively, and the reduction at 100 ppm was statistically significant ($P<0.04$). In males, nobiletin at 100 and 500 ppm reduced the MF by 25 and 45%, respectively, and the reduction at 500 ppm was statistically significant ($P<0.04$). These results indicate that nobiletin suppresses NNK-induced genotoxicity in the lung of *gpt* delta mice.

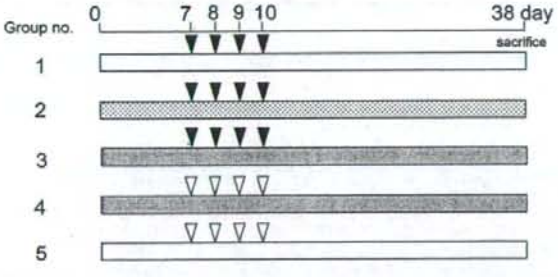

Fig. 1. An experimental design to examine chemopreventive effects of nobiletin against genotoxicity of NNK in the lung of *gpt* delta mice. Twenty female and 25 male eight-week-old *gpt* delta mice were each divided into five groups. Groups 1 through 3 were treated with a single i.p. injection of NNK at a dose of 2 mg/mouse/day for four consecutive days from day 7 through day 10. Groups 2 and 3 were fed diet supplemented with nobiletin at doses of 100 ppm and 500 ppm, respectively, for 38 days. Groups 4 and 5 were treated with saline as vehicle, and Group 4 was fed diet with nobiletin at a dose of 500 ppm for 38 days. Mice were sacrificed at day 38, and the *gpt* MF in the lung were determined. □, basal diet; ▨, nobiletin in diet at a dose of 100 ppm; ■, nobiletin in diet at a dose of 500 ppm; ▼, NNK (2 mg/mouse/day, i.p.); ▽, saline.

Nobiletin inhibits genotoxicity of NNK in the presence of S9 activation in *S. typhimurium* YG7108: To further characterize the suppressive effects of nobiletin against genotoxicity of NNK, we conducted bacterial mutation assays to examine whether nobiletin inhibits genotoxicity of NNK in the presence of S9 activation enzymes (Fig. 2A). NNK at a dose of 500 μg/plate induced mutations in *S. typhimurium* YG7108 and produced about 900 His^+ revertants/plate, which was 40–50 times higher than the value of spontaneous mutations. Nobiletin itself was non-genotoxic either with or without S9 activation (Fig. 2A, C and D).

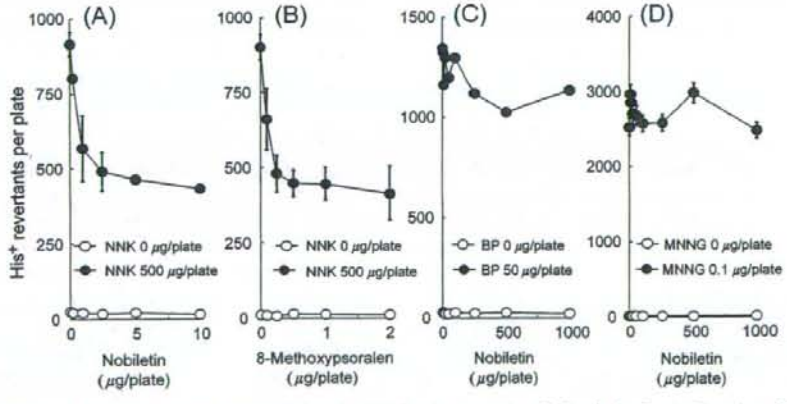

Fig. 2. Suppressive effects of nobiletin against genotoxicity of NNK in the presence of S9 mix in *S. typhimurium* YG7108. Closed circles represent the numbers of His^+ revertants/plate induced by the following compounds: NNK (500 μg/plate) in the presence of S9 mix along with the increasing doses of nobiletin (A), NNK (500 μg/plate) in the presence of S9 mix along with the increasing doses of 8-methoxypsoralen (B); BP (50 μg/plate) in the presence of S9 mix along with the increasing doses of nobiletin (C); MNNG (0.1 μg/plate) in the absence of S9 mix along with the increasing doses of nobiletin. Open circles represent the numbers of His^+ revertants/plate when the non-genotoxicity of nobiletin (A, C and D) and 8-methoxypsoralen (B) were confirmed. Strains used are *S. typhimurium* YG7108 (A, B and D) and *S. typhimurium* YG5161 (C). Averages and standard deviations are presented in A, B and D where three plates were used for the assays. Averages are presented in C where two plates were used for the assay.

Table 1. Suppressive effects of nobiletin against genotoxicity of NNK in the lung of female *gpt* delta mice

Group number*	Animal I.D.	Total colonies	No. of mutants	*gpt* MF ($\times 10^{-6}$)	Average ± S.D.†	*P*-value‡
1	F001	898,500	68	75.7		
NNK alone	F002	1,017,000	57	56.1		
	F003	1,464,000	53	36.2		
	F004	1,054,500	68	64.5		
		4,434,000	246	55.5	58.1 ± 16.7	
2	F005	1,134,000	36	31.8		
NNK	F006	1,353,000	48	35.5		
+ Nobiletin	F007	1,152,000	54	46.9		
(100 ppm)	F008	916,500	37	40.4		
		4,555,500	175	38.4	38.6 ± 6.6	0.036§
3	F009	1,369,500	33	24.1		
NNK	F010	798,000	36	45.1		
+ Nobiletin	F011	1,606,500	66	41.1		
(500 ppm)	F012	1,027,500	48	46.7		
		4,801,500	183	38.1	39.3 ± 10.4	0.052
4	F013	1,059,000	3	2.8		
Nobiletin	F014	1,377,000	4	2.9		
(500 ppm)	F015	1,092,000	6	5.5		
alone	F016	900,000	6	6.7		
		4,428,000	19	4.3	4.5 ± 1.9	<0.001
5	F018	2,856,000	6	2.1		
No treatments	F019	1,560,000	4	2.6		
	F020	1,809,000	9	5.0		
	F021	2,013,000	5	2.5		
		8,238,000	24	2.9	3.0 ± 1.3	<0.001

*Group 1, mice treated with NNK (2 mg/mouse/day × 4 days) alone; Group 2, mice treated with NNK plus nobiletin at a dose of 100 ppm in diet; Group 3, mice treated with NNK plus nobiletin at a dose of 500 ppm in diet; Group 4, mice fed nobiletin at a dose of 500 ppm in diet without NNK treatments; Group 5, mice without treatments with NNK or nobiletin. The Group No. corresponds with group No. in Fig. 1.

†Average ± standard deviation of *gpt* MF of four mice.

‡Differences between *gpt* MF of each group and that of Group 1 were tested for statistical significance using a Student's *t*-test.

§Statistically significant ($P < 0.05$) against Group 1. The values in Groups 4 and 5 are also statistically significant. But the mice in Groups 4 and 5 are not treated with NNK so that the values are not marked with §.

An addition of nobiletin in the reaction mixture containing NNK and S9 mix reduced the genotoxicity of NNK in a dose-dependent manner, and the number of His^+ revertants/plate decreased by more than 50% at the highest dose of nobiletin, i.e., 10 μg/plate. There was no obvious reduction of background lawn of bacteria at any dose of nobiletin, suggesting that nobiletin was not very much toxic under the experimental conditions. Similar dose-dependent reduction of the genotoxicity of NNK was observed with 8-methoxypsoralen (Fig. 2B). An addition of 8-methoxypsoralen into the reaction mixture containing NNK and S9 mix reduced the number of His^+ revertants/plate by more than 50%. Despite the similar inhibitory effects, the dose necessary to reduce the genotoxicity of NNK by 50% was 5- to 10-fold higher with nobiletin than with 8-methoxypsoralen (2.5 μg/plate for nobiletin versus 0.25–0.5 μg/plate for 8-methoxypsoralen). In contrast, nobiletin exhibited weak or virtually no inhibitory effects on the genotoxicity of BP or MNNG, respectively (Fig. 2C and D). An addition of nobiletin reduced the genotoxicity of BP in the presence of S9 activation by 20%, while it did not modulate the genotoxicity of MNNG in the absence of S9 enzymes.

Discussion

Lung cancer continues to be the leading cause of cancer death in developed countries. Dietary compounds with potential to inhibit lung cancer may be a promising and practical approach for reducing the risk of lung cancer caused by smoking. In this study, we examined the chemopreventive efficacy of nobiletin

Table 2. Suppressive effects of nobiletin against genotoxicity of NNK in the lung of male *gpt* delta mice

Group number*	Animal I.D.	Total colonies	No. of mutants	*gpt* MF ($\times 10^{-6}$)	Average ±S.D.†	*P*-value‡
1	M001	960,000	21	21.9		
NNK alone	M002	987,000	32	32.4		
	M003	1,320,000	57	43.2		
	M004	876,000	20	22.8		
	M005	1,892,000	23	12.2		
		6,035,000	153	25.4	26.5±11.8	
2	M007	1,156,000	16	13.8		
NNK	M008	991,000	19	19.2		
+Nobiletin	M009	828,000	20	24.2		
(100 ppm)	M010	828,000	23	27.8		
	M011	840,000	12	14.3		
		4,643,000	90	19.4	19.9±6.1	0.147
3	M013	700,000	16	22.9		
NNK	M014	1,404,000	11	7.8		
+Nobiletin	M015	1,052,000	14	13.3		
(500 ppm)	M016	760,000	10	13.2		
	M017	1,000,000	15	15.0		
		4,916,000	66	13.4	14.4±5.4	0.035§
4	M019	1,028,000	4	3.9		
Nobiletin	M020¶	388,000	4	10.3		
(500 ppm)	M021	1,640,000	6	3.7		
alone	M022	708,000	3	4.2		
	M023	972,000	2	2.1		
		4,348,000	15	3.5	3.5±1.0	0.003
5	M024§	705,000	14	19.9		
No treatments	M025	1,410,000	8	5.7		
	M026	1,410,000	5	3.6		
	M027	1,928,000	3	1.6		
	M028	2,032,000	3	1.5		
		6,780,000	19	2.8	3.1±2.0	0.003

*Group 1, mice treated with NNK (2 mg/mouse/day × 4 days) alone; Group 2, mice treated with NNK plus nobiletin at a dose of 100 ppm in diet; Group 3, mice treated with NNK plus nobiletin at a dose of 500 ppm in diet; Group 4, mice fed nobiletin at a dose of 500 ppm in diet without NNK treatments; Group 5, mice without treatments with NNK or nobiletin. The Group No. corresponds to Group No. in Fig. 1.

†Average ± standard deviation of *gpt* MF of four or five mice.

‡Differences between *gpt* MF of each group and that of Group 1 were tested for statistical significance using a Student's *t*-test.

¶Two unusually high *gpt* MF of M020 and M024 were excluded for the calculation of average by the Smirnov-Grubb's outlier test.

§Statistically significant ($P<0.05$) against Group 1. The values in Groups 4 and 5 are also statistically significant. But the mice in Groups 4 and 5 are not treated with NNK so that the values are not marked with ‖.

against genotoxicity of NNK in the lung of *gpt* delta mice. NNK exposure significantly enhanced the *gpt* MFs in the lung of mice (Tables 1, 2). There was a marked sex difference in the genotoxicity of NNK where females exhibited about twice higher sensitivity than males. This may be due to gender-related differences in the metabolic activation enzymes for NNK (31). The high sensitivity in female than in male mice may be relevant in humans because women are more sensitive to the genotoxic effects of NNK than men (32). Interestingly, dietary administration of nobiletin substantially reduced the *gpt* MFs in both sexes, and the reduction at a dose of 100 ppm in females and 500 ppm in males was statistically significant ($P<0.05$). Administration of nobiletin at 500 ppm also reduced the genotoxicity in females at a similar extent to that observed with nobiletin at 100 ppm. Ikeda *et al.* reported that NNK induces G:C-to-A:T, G:C-to-T:A, A:T-to-T:A, A:T-to-G:C in the lung of *gpt* delta mice (unpublished obervations). Since G:C-to-A:T can activate Ki-*ras* oncogene, the reduction of *gpt* MF may correlate with the reduction of lung tumors (5). Thus, we suggest that nobiletin may be a

chemopreventive agent against NNK-induced lung tumorigenesis in mice. Nobiletin inhibits metastasis (20,21) and suppresses inflammation and promotion (18,33–36). Hence, it may prevent events that occur in multi-step of lung carcinogenesis, i.e., initiation, promotion and progression/metastasis, induced by cigarette smoke. However, certain compounds that can reduce NNK-induced tumors do not necessarily reduce lung tumors in smoke-exposed animals (37). Thus, further examination is needed to evaluate the chemopreventive efficacy of nobiletin against lung tumors induced by cigarette smoke.

In addition to *in vivo* results, we observed reduction of NNK-induced mutations by nobiletin in the present of S9 activation enzymes *in vitro*. Interestingly, nobiletin exhibited a specificity inhibiting the genotoxicity of chemicals in *S. typhimurium*. Although nobiletin inhibited the genotoxicity of NNK, it inhibited the genotoxicity of BP with S9 activation only slightly and did not inhibit the genotoxicity of MNNG without S9 activation. Since MNNG induces O^6-methylguanine leading to G:C-to-A:T mutations (38), we suggest that nobiletin may not enhance the repair activity against O^6-methylguanine or promote error-free translesion bypass across the lesion. Instead, we suggest that nobiletin may suppress the genotoxicity of NNK by inhibiting the activity of CYP (P-450) enzymes involved in the metabolic activation of NNK (39–41). In fact, 8-methoxypsoralen, a specific-inhibitor of CYP2A, similarly suppressed the genotoxicity of NNK in the presence of S9 enzymes (23). The inhibitory effect of nobiletin may be specific to certain CYP enzymes including CYP2A because the genotoxicity of BP, which is activated *via* CYP1A1 (42), was weakly inhibited by nobiletin. However, since both nobiletin and 8-methoxypsoralen inhibited the genotoxicity of NNK only by 50%, we suggest that other CYP enzymes may be responsible for the remaining genotoxicity of NNK in the S9 enzymes. Although nobiletin did not effectively affect the genotoxicity of BP in the present study, Conney *et al.* (43) observed that nobiletin stimulates human liver microsomes and activates both the hydroxylation of BP and the metabolism of aflatoxin B_1 to mutagens. Nobiletin also stimulates oxidative metabolism of zoxazolamine by rat liver microsomes (44) and acetaminophen by human liver microsome (45). These reports suggest that nobiletin has a potential to modulate CYP enzyme activities.

In summary, we examined the chemopreventive efficacy of nobiletin against the genotoxicity of NNK in the lung of female and male *gpt* delta mice. Dietary administration of nobiletin significantly reduced the genotoxicity of NNK in both sexes. In addition, the chemical was able to reduce NNK-induced genotoxicity in *S. typhimurium* YG7108 in the presence of S9 activating enzymes. Our findings suggest that nobiletin could inhibit the activities of certain CYP enzymes involved in the metabolic activation of NNK, thereby suppressing the genotoxicity in the lung of mice.

Acknowledgements: This work was supported in part by Grants-in-Aid for Cancer Research from the Ministry of Health, Labour and Welfare of Japan and the Tutikawa Memorial Fund for Study in Mammalian Mutagenicity.

References

1 Tobacco smoking. IARC Monogr Eval. Carcinog. Risk Chem. Hum. 1986; 38: 35–394. Lyon, France, International Agency for Research on Cancer.
2 Hecht SS, Carmella SG, Foiles PG, Murphy SE. Biomarkers for human uptake and metabolic activation of tobacco-specific nitrosamines. Cancer Res. 1994; 54: 1912s–17s.
3 Hecht SS, Hoffmann D. Tobacco-specific nitrosamines, an important group of carcinogens in tobacco and tobacco smoke. Carcinogenesis. 1988; 9: 875–84.
4 4-(Methylnitrosamino)-1-(3-pyridyl)-1-butanone (NNK). IARC Monogr Eval. Carcinog. Risk Chem. Hum. 1985; 37: 209–23. Lyon, France, International Agency for Research on Cancer.
5 Ronai ZA, Gradia S, Peterson LA, Hecht SS. G to A transitions and G to T transversions in codon 12 of the Ki-ras oncogene isolated from mouse lung tumors induced by 4-(methylnitrosamino)-1-(3-pyridyl)-1-butanone (NNK) and related DNA methylating and pyridyloxobutylating agents. Carcinogenesis. 1993; 14: 2419–22.
6 Hecht SS. DNA adduct formation from tobacco-specific *N*-nitrosamines. Mutat Res. 1999; 424: 127–42.
7 Hecht SS. Chemoprevention of lung cancer by isothiocyanates. Adv Exp Med Biol. 1996; 401: 1–11.
8 Hecht SS. Approaches to chemoprevention of lung cancer based on carcinogens in tobacco smoke. Environ Health Perspect. 1997; 105 Suppl 4: 955–63.
9 Thapliyal R, Maru GB. Inhibition of cytochrome P450 isozymes by curcumins *in vitro* and *in vivo*. Food Chem Toxicol. 2001; 39: 541–7.
10 Prokopczyk B, Rosa JG, Desai D, Amin S, Sohn OS, Fiala ES *et al.* Chemoprevention of lung tumorigenesis induced by a mixture of benzo(a)pyrene and 4-(methylnitrosamino)-1-(3-pyridyl)-1-butanone by the organoselenium compound 1,4-phenylenebis(methylene)selenocyanate. Cancer Lett. 2000; 161: 35–46.
11 Li L, Xie Y, El Sayed WM, Szakacs JG, Franklin MR, Roberts JC. Chemopreventive activity of selenocysteine prodrugs against tobacco-derived nitrosamine (NNK) induced lung tumors in the A/J mouse. J Biochem Mol Toxicol. 2005; 19: 396–405.
12 Weitberg AB, Corvese D. Effect of vitamin E and beta-carotene on DNA strand breakage induced by tobacco-specific nitrosamines and stimulated human phagocytes. J Exp Clin Cancer Res. 1997; 16: 11–4.
13 Nishino H, Tokuda H, Satomi Y, Masuda M, Osaka Y, Yogosawa S *et al.* Cancer prevention by antioxidants.

Biofactors. 2004; 22: 57–61.
14 Lantry LE, Zhang Z, Crist KA, Wang Y, Hara M, Zeeck A *et al.* Chemopreventive efficacy of promising farnesyltransferase inhibitors. Exp Lung Res. 2000; 26: 773–90.
15 Lee HY, Oh SH, Woo JK, Kim WY, Van Pelt CS, Price RE *et al.* Chemopreventive effects of deguelin, a novel Akt inhibitor, on tobacco-induced lung tumorigenesis. J Natl Cancer Inst. 2005; 97: 1695–9.
16 Minagawa A, Otani Y, Kubota T, Wada N, Furukawa T, Kumai K *et al.* The citrus flavonoid, nobiletin, inhibits peritoneal dissemination of human gastric carcinoma in SCID mice. Jpn J Cancer Res. 2001; 92: 1322–8.
17 Suzuki R, Kohno H, Murakami A, Koshimizu K, Ohigashi H, Yano M *et al.* Citrus nobiletin inhibits azoxymethane-induced large bowel carcinogenesis in rats. Biofactors. 2004; 22: 111–4.
18 Murakami A, Nakamura Y, Torikai K, Tanaka T, Koshiba T, Koshimizu K *et al.* Inhibitory effect of citrus nobiletin on phorbol ester-induced skin inflammation, oxidative stress, and tumor promotion in mice. Cancer Res. 2000; 60: 5059–66.
19 Kohno H, Yoshitani S, Tsukio Y, Murakami A, Koshimizu K, Yano M *et al.* Dietary administration of citrus nobiletin inhibits azoxymethane-induced colonic aberrant crypt foci in rats. Life Sci. 2001; 69: 901–13.
20 Miyata Y, Sato T, Yano M, Ito A. Activation of protein kinase C betaII/epsilon-c-Jun NH2-terminal kinase pathway and inhibition of mitogen-activated protein/extracellular signal-regulated kinase 1/2 phosphorylation in antitumor invasive activity induced by the polymethoxy flavonoid, nobiletin. Mol Cancer Ther. 2004; 3: 839–47.
21 Kawabata K, Murakami A, Ohigashi H. Nobiletin, a citrus flavonoid, down-regulates matrix metalloproteinase-7 (matrilysin) expression in HT-29 human colorectal cancer cells. Biosci Biotechnol Biochem. 2005; 69: 307–14.
22 Takanaga H, Ohnishi A, Yamada S, Matsuo H, Morimoto S, Shoyama Y *et al.* Polymethoxylated flavones in orange juice are inhibitors of P-glycoprotein but not cytochrome P450 3A4. J Pharmacol Exp Ther. 2000; 293: 230–6.
23 Miyazaki M, Yamazaki H, Takeuchi H, Saoo K, Yokohira M, Masumura K *et al.* Mechanisms of chemopreventive effects of 8-methoxypsoralen against 4-(methylnitrosamino)-1-(3-pyridyl)-1-butanone-induced mouse lung adenomas. Carcinogenesis. 2005; 26: 1947–55.
24 Yamada M, Matsui K, Sofuni T, Nohmi T. New tester strains of *Salmonella typhimurium* lacking O^6-methylguanine DNA methyltransferases and highly sensitive to mutagenic alkylating agents. Mutat Res. 1997; 381: 15–24.
25 Yamada M, Sedgwick B, Sofuni T, Nohmi T. Construction and characterization of mutants of *Salmonella typhimurium* deficient in DNA repair of O^6-methylguanine. J Bacteriol. 1995; 177: 1511–9.
26 Tsukayama T, Kawamura Y, Ishizuka T, Hayashi S, Torii F. Improved, rapid and efficient synthesis of polymethoxyflavones under microwave irradiation and their inhibitory effects on melanogenesis. Heterocycles. 2003; 60: 2775–84.
27 Nohmi T, Suzuki T, Masumura K. Recent advances in the protocols of transgenic mouse mutation assays. Mutat Res. 2000; 455: 191–215.
28 Nohmi T, Masumura K. Molecular nature of intrachromosomal deletions and base substitutions induced by environmental mutagens. Environ Mol Mutagen. 2005; 45: 150–61.
29 Maron DM, Ames BN. Revised methods for the Salmonella mutagenicity test. Mutat Res. 1983; 113: 173–215.
30 Matsui K, Yamada M, Imai M, Yamamoto K, Nohmi T. Specificity of replicative and SOS-inducible DNA polymerases in frameshift mutagenesis: mutability of *Salmonella typhimurium* strains overexpressing SOS-inducible DNA polymerases to 30 chemical mutagens. DNA Repair (Amst). 2006; 5: 465–78.
31 Schulze J, Schlager W, Wunsch R, Richter E. Metabolism of 4-(methylnitrosamino)-1-(3-pyridyl)-1-butanone (NNK) by hamster, mouse and rat intestine: relevance of species differences. Carcinogenesis. 1996; 17: 1093–9.
32 Hill CE, Affatato AA, Wolfe KJ, Lopez MS, Hallberg CK, Canistro D *et al.* Gender differences in genetic damage induced by the tobacco-specific nitrosamine NNK and the influence of the Thr241Met polymorphism in the XRCC3 gene. Environ Mol Mutagen. 2005; 46: 22–9.
33 Murakami A, Nakamura Y, Ohto Y, Yano M, Koshiba T, Koshimizu K *et al.* Suppressive effects of citrus fruits on free radical generation and nobiletin, an anti-inflammatory polymethoxyflavonoid. Biofactors. 2000; 12: 187–92.
34 Sato T, Koike L, Miyata Y, Hirata M, Mimaki Y, Sashida Y *et al.* Inhibition of activator protein-1 binding activity and phosphatidylinositol 3-kinase pathway by nobiletin, a polymethoxy flavonoid, results in augmentation of tissue inhibitor of metalloproteinases-1 production and suppression of production of matrix metalloproteinases-1 and -9 in human fibrosarcoma HT-1080 cells. Cancer Res. 2002; 62: 1025–9.
35 Lin N, Sato T, Takayama Y, Mimaki Y, Sashida Y, Yano M *et al.* Novel anti-inflammatory actions of nobiletin, a citrus polymethoxy flavonoid, on human synovial fibroblasts and mouse macrophages. Biochem Pharmacol. 2003; 65: 2065–71.
36 Ohnishi H, Asamoto M, Tujimura K, Hokaiwado N, Takahashi S, Ogawa K *et al.* Inhibition of cell proliferation by nobiletin, a dietary phytochemical, associated with apoptosis and characteristic gene expression, but lack of effect on early rat hepatocarcinogenesis *in vivo*. Cancer Sci. 2004; 95: 936–42.
37 Witschi H. Successful and not so successful chemoprevention of tobacco smoke-induced lung tumors. Exp Lung Res. 2000; 26: 743–55.
38 Loechler EL, Green CL, Essigmann JM. *In vivo* mutagenesis by O^6-methylguanine built into a unique site in a viral genome. Proc Natl Acad Sci USA. 1984; 81: 6271–5.
39 Fujita K, Kamataki T. Predicting the mutagenicity of tobacco-related *N*-nitrosamines in humans using 11